HIV-1 strain-specific neutralizing antibody responses and the dynamics of viral evolution

LERATO CHARLOTTE MAJARA

This dissertation is submitted in fulfilment of the requirements for the degree of Master of Science in the Division of Medical Virology, Department of Pathology in the Faculty of Health Sciences at the University Of Cape Town

Supervisor: Professor Carolyn Williamson

Co-supervisor: Dr Colin Anthony

Jan 2016

Table of contents

List of figures

List of tables

Abstract

It is widely held that for an HIV-1 vaccine to provide sterilizing immunity, it would need to elicit broadly neutralizing antibodies (bnAbs). However, factors underlying the development of these antibodies are not clear. There is evidence to suggest that in some individuals who develop bnAbs, the development of breadth is influenced by the co-evolution of the transmitted/founder (t/f) virus and earlier strain-specific neutralizing antibody (ssnAb) responses. Here we characterized the viral evolution, ssnAb and bnAbs responses in CAP292, an HIV-1 infected woman who developed bnAb responses from one year post infection.

We used single genome amplification (SGA) to characterize viral evolution at four time points: at acute infection; after the development of strain-specific neutralizing responses; at the first detection of the broadly neutralizing antibody response; and lastly, at the peak of the broad response. We identified the t/f virus, and generated chimeric viruses from this to determine the targets of the ssnAb responses. A panel of site-directed mutant viruses were used to map the specificity of the bnAb responses.

Our data indicated that infection was most likely founded by a single virus and that the first wave of ssnAbs emerged at 14 weeks post infection (w.p.i), targeting the V1V2 loop of Envelope (Env). A second wave of ssnAbs, possibly targeting the C3V4 region, emerged by 30 w.p.i. Two distinct viral clusters were detected by the time the bnAb response peaked, suggesting the presence of distinct escape pathways. Mapping of the bnAb specificities indicated that CAP292 produced PGT128-like bnAb responses targeted toward the 332 glycan.

These data illustrate that an early ssnAb response emerged towards the C3V4 region, with a later bnAb response possibly targeting the C3 glycan at position 332. Further

work is required to confirm the target of the bnAbs and determine whether there was a link between the earlier ssnAb targets and later bnAb specificities in CAP292.

Abbreviations

µg	microgram
µl	microlitre
Ad5	adenovirus serotype 5
ADCC	antibody-dependent cellular cytotoxicity
aHD	average Hamming Distance
ARV	antiretroviral
bnAb	broadly neutralizing antibodies
ºC	Degrees celsius
CAPRISA	Centre for the AIDS Programme of Research
CCR5	C-C chemokine receptor type 5
CD4	cluster of differentiation 4
cDNA	complementary DNA
cPCR	colony polymerase chain reaction
CTL	cytotoxic T lymphocytes
CXCR4	C-X-C chemokine receptor type 4
DMEM	Dulbecco's modified eagle medium
DNA	deoxyribonucleic acid
E. coli	*Escherichia coli*
EDTA	ethylenediamine tetraacetic acid
Env	Envelope protein
env	envelope gene

GALT	gut-associated lymphoid tissue
gp	glycoprotein
HCDR	heavy chain complementarity determining region
HD	hamming distance
HEK	human embryonic kidney
HIV	Human immunodeficiency virus
HLA	human leukocyte antigen
HR	heptide repeat region
ID	Infectious dose
IFN	interferon
IL	interleuken
indels	insertions or deletions
kb	kilobases
LB	Luria-Bertani broth
$MgCl_2$	magnesiumm chloride
min	minutes
ml	millilitre
mM	millimolar
MPER	membrane proximal external region
MSM	men who have sex with men
nAb	neutralizing antibodies
ng	nanogram

NHP	non-human primate
NICD	National Institute of Communicable Diseases
NKT	natural killer T cells
nnAb	non-neutralizing antibodies
PCR	polymerase chain reaction
pH	hydrogen potential
PNLG	potential N-linked glycosylation site
RLU	relative luminescence units
RNA	ribonucleic acid
s	seconds
SD	standard deviation
SGA	single genome amplification
SHIV	SIV and HIV chimeric virus
SIV	Simian immunodeficiency virus
ssnAb	strain-specific neutralizing antibodies
t/f	transmitted/founder
TAE	Tris-acetate acid EDTA
TasP	treatment as prevention
Tat	transcriptional transactivator protein
TCID	tissue culture infectious dose
UCA	unmutated common ancestor
UV	ultra violet

v/v	volume per volume
w.p.i	weeks post infection
w/v	weight per volume

Declaration

I, Lerato Charlotte Majara hereby declare that the work on which this dissertation/thesis is based is my original work (except where acknowledgements indicate otherwise) and that neither the whole work nor any part of it has been, is being, or is to be submitted for another degree in this or any other university.

I empower the university to reproduce for the purpose of research either the whole or any portion of the contents in any manner whatsoever.

Signature:

Signed by candidate

Date: 14. Jan. 2016

Acknowledgements

I'd like to thank the following people and organisations for the encouragment and support in completing this degree:

My supervisor Professor Carolyn Williamson. Thank you Prof for providing me the opportunity to learn and grow (personally and academically) in your lab.

My co-supervisor, Dr Colin Anthony for your assistance and guidance.

My mother for driving me to finish this work. You didn't quite understand why it was taking so long. Thank you for standing by me anyway.

My friends Tembeka Sineke and Asanda Mtintsilani for being inspirational. We walked the same journey, although on different paths. Thank for you understanding when 'I didnt' want to talk about it'.

The Council of Scientific and Industrial Research (CSIR) and Poliomyelitis Research Foundation (PRF) for providing the financial support.

Dr Maribanyane Nonyane from the writing centre for reading and re-reading my thesis several times and providing a way forward.

Dr Melissa Abrahams for her patience and readiness to help.

The HIV diversity and pathogenesis group in general.

1 Literature review

1.1 Introduction

Since its discovery in 1983, the HIV-1 epidemic has expanded with 36.9 million people living with HIV-1 in 2014 [1]. While there are several HIV-1 subtypes and circulating recombinant forms, subtype C makes up 56% of the pandemic and is responsible for the overwhelming majority of infections in South Africa [2]. About 18% of the South African adult population (15-49 years old) are living with HIV-1. Although prevalence has stabilized, the global 2 million new infections in 2014 indicate that the epidemic is far from over [1].

It is well established that antiretroviral drugs (ARVs) prevent mother to child HIV-1 transmission [3] [4], and more recently treatment as prevention (TasP) is being used as an available intervention method to reduce sexual transmission of HIV-1. There is ample evidence to support TasP in HIV-1 negative individuals: firstly, ARVs when used as pre-exposure prophylaxis reduce HIV-1 acquisition rates in men who have sex with men (MSM) [5] and in discordant heterosexual couples [6] [7] [8] [9] [10] [11] [12]; and in one study topical application of ARV-based microbicides reduced HIV-1 acquisition in women [13]. The use of ARV-based microbicides in HIV-1 prevention has not been reproduced in other clinical trials [14] [15]. Treatment of HIV-1 infected individuals can reduce transmission by 96% [6] and the global benefit of TasP is that the treatment of a large proportion of HIV-1 infected individuals has the potential to reduce the HIV-1 'community viral load' and subsequently reduce the chance of HIV-1 transmission at a population level [16] [17] [18].

However, TasP has limitations that may prevent its full effectiveness: (i) access to treatment is not universal; for instance, in 2013 only 2.6 million of the 6.8 million were receiving treatment in South Africa [19], (ii) the scale of the required roll-out for supply of medications has a negative financial implication; especially for the economies of developing countries [20] [21], (iii) there may be low adherence to medication due to adverse drug reactions , socio-economic status, social stigma and other psychosocial conditions (e.g. drug and alcohol use, depressive symptoms, anxiety symptoms) [22] [23] [24] [25], (iv) ultimately low adherence may lead to drug resistance [26], which is in itself a limitation of TasP.

Vaccines are the most effective way to control viral pandemics [27] and offer a solution to the limitations of TasP. Through reducing number of new infections and providing herd immunity, vaccines can ultimately lead to the eradication of the HIV-1 epidemic.

1.2 HIV-1 vaccine trials

Although there is no effective vaccine against HIV-1 acquisition, four vaccine concepts have been tested in large proof of concept (Phase 2b) or efficacy trials (Phase 3) including: protein subunit proteins (VAX003 and VAX004); Ad5 vaccine vectors (HVTN502 and HVTN503), poxvirus vector prime protein boost (RV144); and DNA prime Ad5 vector boost approaches (HVTN 505). The trial dates are shown in **Figure 1.1**.

The first Phase 3 efficacy trials were conducted between 1998 and 2003. The VAX004 and VAX003 trials investigated the use of HIV-1 subunit proteins to elicit a neutralizing antibody response to prevent HIV-1 infection. VAX004 used a recombinant gp120

from subtype B viruses, while VAX003 used subunits from subtypes B and E. These trials were conducted in an MSM population and heterosexual women at high risk of HIV-1 infection. A weak neutralizing antibody response was mounted in both trials, which was only effective against highly neutralization sensitive viruses and did not protect against infection. Therefore, these vaccines showed no efficacy [28] [29].

Between 2004 and 2007, the second concept tested was the induction of T cell-mediated responses to reduce viral load and delay clinical disease progression. The STEP/HVTN502 and Phambili/HVTN503 Phase 2b trials tested this concept by using a replication-deficient vector Adenovirus serotype 5 (Ad5) encoding HIV-1 subtype B *gag, nef* and *pol* genes [30]. STEP was conducted largely in a population of MSM from North America, South America and Australia and included high-risk heterosexual men and women from the Caribbean. Phambili was conducted in South Africa in a heterosexual population. The lack of vaccine efficacy resulted in termination of both studies. Of concern was the finding that HIV-1 susceptibility was increased in men who had pre-existing immunity to Ad5 and were uncircumcised in the STEP trial. In both trials, the vaccine failed to lower viral load and delay disease progression in those who became infected [30] [31]. Although the vaccine elicited T-cell responses, they were narrow and only targeted one to three epitopes [32].

A third concept tested aimed to elicit both T cell responses and neutralizing antibodies was and was evaluated in the RV144 trial in Thailand [33]. This trial was conducted using the prime-boost strategy. The vaccine candidate prime was a canarypox vector containing HIV-1 subtype B *gag*, *pol* and *env (*envelope) genes. The boost contained a recombinant of gp120 containing subunits from HIV-1 subtypes B and E. Although the vaccine had no effect on the peak viremia after infection, HIV-1 acquisition was

reduced by 31% [33]. A correlate of risk analysis showed the vaccine recipients who did not acquire infection had V2 loop Env binding antibodies [34]. This suggests that inducing anti-HIV antibodies targeting the V1V2 loops may be important in preventing infection.

Lastly, the HVTN505 Phase 2b trial was conducted between 2009 and 2013 [35]. The trial was conducted in MSM or transgendered women who have sex with men in the United States of America (USA). A prime-boost strategy to elicit both T cell-mediated responses and neutralizing antibodies was employed. The vaccine regimen contained a prime that was made up of a DNA plasmid containing *env* from subtype A, B and C, and *gag*; *pol* and *nef* genes from subtype B. The boost comprised a recombinant Adenovirus serotype 5 (Ad5) vector containing *env* from subtype A ,B and C, as well as *gag* and *pol* from subtype B [35]. Similarly, the vaccine failed to protect against acquisition of infection and did not lower viral load post acquisition.

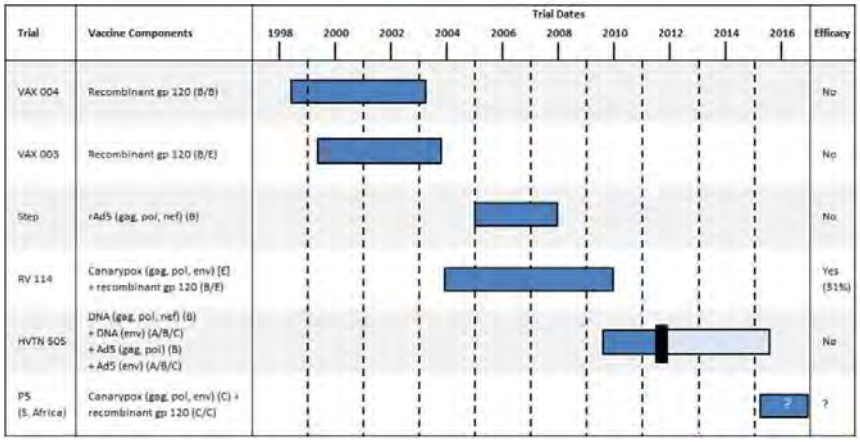

Figure 1.1. HIV-1 Human Vaccine Clinical Trials. An illustration of four concepts tested in five human clinical trials conducted to date. The trial name, vaccine antigens and the year of initiation and termination of the trials are

indicated. The HVTN505 Trial was initiated in 2009, and was meant to progress into 2015. This was halted (black bar) in 2013 (Figure from Esparza *et al*. [36]).

1.3 Why neutralizing antibodies are important

Neutralizing antibodies (nAbs) are a known correlate of protection in most licensed vaccines (reviewed by Plotkin [27]) and provide sterilizing immunity against SIV in non-human primates [37]. nAbs lag behind the high rate of mutation and immune escape by the virus rendering them ineffective against contemporaneous viruses (reviewed by Mascola [38]). Moreover, the high level of viral diversity results in early antibodies that are only able to target a portion of the viral population that elicited them, and are thus strain-specific. Antibodies that are able to neutralize HIV from different individuals are known as broadly neutralizing antibodies (bnAbs) and have been isolated from chronically infected individuals. Studies have shown that passive transfer of bnAbs in nonhuman primates protects against infection [39 37 40]. Additionally, administration of a cocktail of these antibodies suppresses viral replication in rhesus monkey chronically infected with SHIV (an SIV and HIV-1 chimeric virus) depending on the viral load during the time of administering the antibodies [41]. To date no vaccine has been able to elicit bnAbs. Current research is focused on elicitation of broadly neutralizing antibodies through vaccination, via a pathway that mimics natural infection (reviewed later) in the hope that this will prevent HIV-1 infection in vaccinees.

1.4 HIV-1 envelope architecture

To better understand the interaction between antibodies and the virus, it is essential to understand the architecture of the HIV-1 envelope protein (Env), as it is the target for

neutralizing antibodies. Env, comprises heterodimers of non-covalently bound surface gp120 and transmembrane gp41 (gp: glycoprotein). The gp41 is anchored to the membrane by a 7-stranded-β–sandwich [42]. The heterodimers are arranged as trimers also known as 'spikes' on the viral membrane [43].

The gp120 is made up of a highly glycosylated outer domain, bridging sheet and an inner domain (**Figure 1.2**). The outer domain is made up of five variable loops -V1, V2, V3, V4 and V5; with the more conserved constant domains (C1, C2, C3, C4 and C5) make up the inner domain [44] [45]. Three of the variable loops, V1, V2, V3 form an association domain at the apex of the spike that stabilizes the conformation of the envelope protein (Env). The amino acid residues necessary for the binding of the infection co-receptor are found in V3 and the bridging sheet, linking V1V2 with V3. The role of the V4 and V5 have not been clearly defined, but may be targets for neutralizing antibodies and/or mask regions of antibody sensitivity. The C2, C3 and C4 domains form a hydrophobic cavity that makes up the CD4-binding site [46]. The three monomers of gp41 form a mushroom-like shape at the base of gp120. Gp41 is made up of an ectodomain on the N-terminus and a transmembrane domain on the C-terminus. The ectodomain contains two heptad repeat regions (HR1 and HR2), membrane-proximal external region (MPER) and a hydrophobic fusion peptide. All components are necessary for the fusion of the viral and cellular membranes during HIV-1 infection.

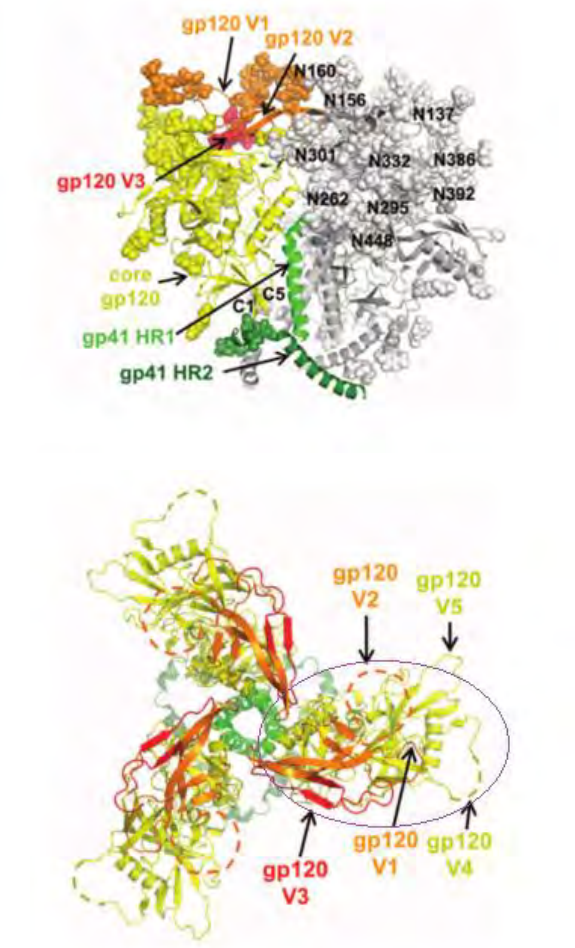

Figure 1.2. Architecture of HIV-1 Envelope. The core gp120 is shown in yellow, the V1V2 in orange and V3 in red. The components of gp41 are shown in different shades of green. **A**. Side view of the HIV trimer. One of the three protomers is shown in colour, while the other two are shown as a gray mash. Glycans are shown as spheres. **B**. Top view of HIV trimer. The components of gp120 are indicated on the encircled protomer (Figure from Julien *et al*. [167]).

1.5 Envelope mediates entry into target cells

The HIV-1 Env spike transitions between three distinct conformations to allow viral entry into the host cell- pre-fusion, intermediate and post-fusion. The pre-fusion, also known as 'native' Env conformation is described above. Here, we review the conformational changes that occur, leading to the entry of viral genetic material into the host targeted cells (**Figure 1.3**).

The first conformational changes occur upon binding of CD4, to the viral CD4-binding site located in the hydrophobic cavity formed in the gp120 inner domain. The gp120 bridging sheet undergoes changes to become a 4-stranded-β-sheet. The V3 dissociates from the V1V2 loop and extends away from the spike, toward the target cell membrane. Both the bridging sheet and the V3 orientate towards the cellular membrane to initiate co-receptor binding. A cavity is then formed wherein the cellular co-receptor (CCR5) binds [47] [48] [49]. The major co-receptors for HIV-1 binding are chemokine receptors CCR5 and CXCR4. The bridging sheet comes into contact with the co-receptor followed by the V3 loop [50] [51]. This induces conformational changes in gp41, leading to the formation of a six-helical bundle by rearrangement of HR1 and HR2. This brings the cellular and viral membrane into close proximity. A fusion pore is initiated, through which the viral capsid can enter the cell [52] [53].

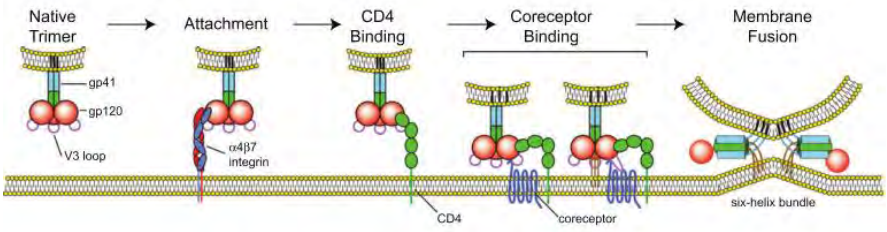

Figure 1.3. Viral entry into target cells. HIV-1 first initiates contact with the target cell by binding to the α4β7 integrin**.** The CD4 binding site on the HIV-1 gp120 then binds to CD4 expressed on the target cell. This binding results in conformational changes in the gp120 resulting in exposure of the V3 co-receptor binding site. The V3 loop interacts with the CCR5 co-receptor on the target cell. Following this engagement with the co-receptor, the gp120 undergoes further conformational changes which facilitate the insertion of the gp41 fusion peptide into the host membrane. HR1 and HR2 consequently interact to form a six-helix bundle which brings the viral and host membranes into close proximity. A fusion pore is formed allowing entry of the HIV-1 capsid into the target cell (Figure from Haqqani & Tilton [54]).

Viral entry is the first step of the viral replication cycle. Described below are the events that occur once infection is established and immune responses emerge.

1.6 HIV-1 transmission bottleneck and expansion of transmitted/founder virus.

Sexual transmission of HIV-1 occurs when either cell free or cell associated virus crosses the mucosal epithelium through transcytosis, direct contact with CD4+ T cells or migration through intercellular spaces [55] [56]. The epithelium acts as a 'genetic bottleneck', allowing only one, or a few, viral variants through the mucosal barrier to establish infection in the new recipient [57] [58] [59]. About 80% of transmission events that result in clinical infection are by a single viral variant, owing to the severity of the transmission bottleneck [60] [61] [62]. In the other 20%, infection is caused by between two to five closely related variants [60]. The virus that establishes infection is known as the

transmitted/founder virus (t/f) and has properties such as common usage of CCR5 (co)-receptor to infect target cells, and in HIV-1 subtypes A and C infection, transmitted viruses have shorter variable loops and fewer number of potential N-linked glycosylation sites (PNLGs), when compared to the variants that emerge later on during infection [63] [64] [65] [66] [67] [68].

During acute infection, the t/f virus replicates exponentially to reach peak viremia, generating genetic derivatives collectively referred to as a quasispecies [69]. The quasispecies population in early infection is relatively homogenous, has low diversity, a Poisson distribution of hamming distances and a star-like phylogeny typifying infection by a single viral variant [60] [61]. Deviations from the model would suggest multiplicity of infection greater than one.

Local replication at the site of infection is followed by exponential expansion of the viral pool, disseminating virus to the local draining lymph nodes and gut-associated lymphoid tissue (GALT). During this stage, there is high CD4 T cell depletion and extensive damage to the lymphoid tissue [70]. This is followed by a sharp decline in viral load over the next weeks, to a level of viral load 'set point' - a level where viral replication is maintained at a semi steady state.

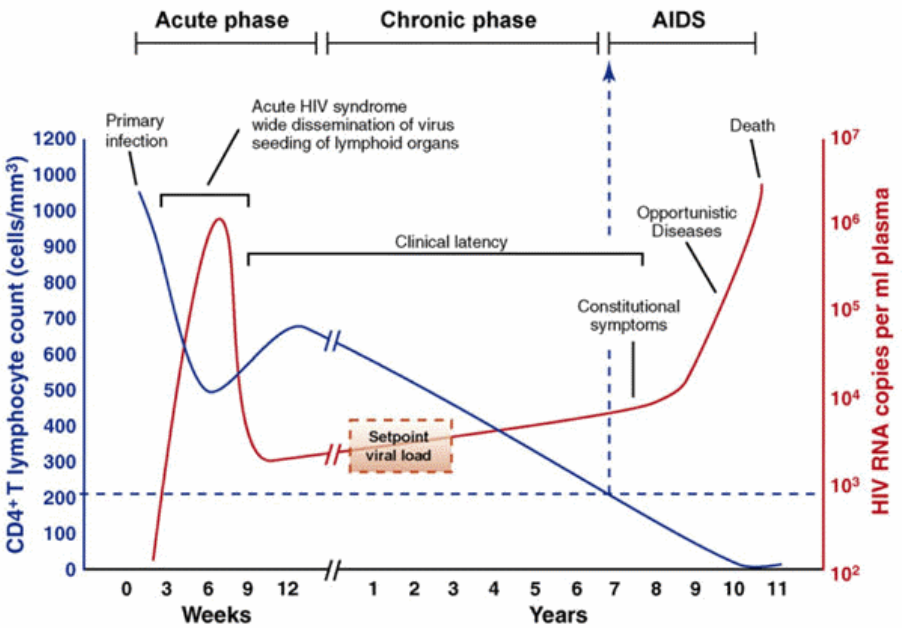

Figure 1.4. Clinical stages of HIV-1 infection. The red and blue curves show the viral load and CD4+ T cell count, respectively, during the different stages of HIV-1 infection. Acute phase stage is marked by an exponential increase in viral load, and rapid decline in CD4T+ cell count. Viral set point is reached and maintained in the chronic phase (Figure from 2014.igem.org [71]).

1.7 Immune responses to HIV-1

This combination of viral replication, dissemination and tissue damage in the early stages of infection results in immune activation and the development of HIV-specific immune responses (reviewed Appay & Sauce [72]) [73]. Here, we review HIV-1 in the context of the different immune responses elicited. We also assess the relevance of the different responses as correlates of acquisition risk in vaccine trials.

1.7.1 Innate immune response

The innate immune response is the first line of defense against infection and thus the first response to interact with HIV-1. Several systems constitute this response: the epithelial barrier, complement system, inflammatory cytokines, and phagocytic cells. The early immune stimulation results in the activation of these systems.

The response is characterized by production of various cytokines and chemokines, an increase in acute-phase proteins and activation of Natural Killer T (NKT) cells [74]. NKT, are expanded during infection and function by killing virally infected cells through the production of granzymes. The production of acute-phase proteins is triggered by the release of pro-inflammatory cytokines such as interleukin-1 (IL-1). Interferons (IFN) have antiviral activity and therefore provide a mechanism for control of HIV-1 replication and has been associated with reduced viral load and rate of disease progression [75] [76] [77] [78] [79]. Host restriction factors have also shown to play an important role in controlling HIV infection including tripartite motif containing protein (TRIMs), and cytosine deaminase protease among others [80].

However, the immune activation does not always have the desired effect. The cytokine storm that results from chronic immune activation, recruits susceptible CD4+ T cells, or dendritic cells to site of infection, which may facilitate spread of the virus to uninfected cells [74] [81]. Chronic immune activation has also been shown to increase susceptibility to HIV-1 acquisition in South African women [82] [83].

1.7.2 Adaptive immune responses

The adaptive immune response is made up of two arms: the cell-mediated and antibody immunity.

1.7.2.1 Cell-mediated responses

The earliest responses shown to have an impact on HIV-1 replication are cytotoxic T-lymphocyte cell (CTL) (or CD8+ T cells) which arise just days after infection, before development of the first antibodies [74] [84]. The peak in these responses coincides with the decline in viremia, suggesting that CTLs inhibit HIV-1 replication. The earliest targets of the CTLs are the viral proteins Nef and the highly variable Env. The more conserved proteins such as Gag and Pol are targeted at a later stage [84] [85].

Key viral sequence changes that occur as viral load decreases are often associated with CTL responses, and are referred to as CTL escape [86] [87]. Escape occurs as single or multiple amino acid changes in the T-cell receptor, HLA binding site, or processing mutations, and render the mutant viruses resistant to CTL cell responses. Escape may, however, result in reduced replicative potential of the virus when occurring in the conserved regions (e.g Gag) [88] [89].

Studies in nonhuman primates highlight the importance of CTLs for vaccine development. CTLs reduced viremia in challenged macaques, and depletion of CD8+ T cells resulted in increased viral load, showing that CD8+ T cells were responsible for limiting viral replication [90] [91]. Additionally, a vaccine candidate RhCMV provided long-term control of Rhesus macaques and even cleared infection in 55% of macaques. This protection was associated with non-classical SIV-specific

CD8+ T cells responses including MHC-II and MHC-E responses, showing the impact of the cells on HIV pathogenesis [92]. However, vaccine studies in humans have been unsuccessful in proving the effectiveness of these responses, either in preventing infection or in reducing viremia after infection was established, as seen in the STEP trial [32].

1.7.2.2 Non-neutralizing antibodies

The first antibodies against HIV-1 proteins are detectable approximately 13 days (ranging from 10 -17 days) post infection in all infected individuals (**Figure 1.5**) and are usually non-neutralizing [93] [94]. This means that they bind to viral proteins, but do not block viral entry into cells. They recruit other cells of the innate response such as phagocytes, and activate the complement system allowing killing of the virus through either complement-mediated lysis, opsonisation by phagocytes or antibody-dependent cellular cytotoxicity (ADCC) [95]. High levels of ADCC-mediating non-neutralizing antibodies (nnAb) are associated with the maintenance of low viral loads in HIV-1 elite controllers [96]. Although they may provide clinical benefit, the presence of ADCC-mediating antibodies during acute infection does not reduce viremia over this phase of infection [94].

However, the RV144 trial showed that binding antibodies targeting the V1V2 loop were associated with the 31% efficacy of the vaccine [34]. These antibodies were shown to mediate ADCC by targeting conserved regions in V2 [97] [98]. Additionally, sieve analysis of the viral sequences from vaccine compared to placebo breakthrough infections, showed that vaccine efficacy was improved when the viral sequences matched the sequence of the vaccine *env* insert at position 169 and did not match at position 181.

The vaccine efficacy was 48% when the amino acid residue at 169 was lysine (K), and 78% when the residue at 181 was not an Isoleucine (I) [99]. A monoclonal antibody (CH58) isolated from a vaccine recipient, showed ADCC activity that targeted K169 [100]. These data showed that amino acid residues in the V2 play a role in HIV-1 susceptibility and that non-neutralizing immune responses to this region were associated with reduced risk of infection. Due to the overall low efficacy of the vaccine, some researchers are suggesting that the non-neutralizing response should be complemented by neutralizing antibodies, thus forming a synergistic relationship to prevent infection [101].

1.7.2.3 Strain-specific neutralizing antibodies

Neutralizing antibodies prevent infection of cells by binding to regions of the envelope trimer important for entry. The earliest neutralizing antibodies to develop during HIV-1 infection are known as strain-specific neutralizing antibodies (ssnAbs), and are usually detectable approximately 12 weeks after HIV-1 acquisition and may continue to emerge throughout the course of infection (**Figure 1.5**) [102]. These antibodies are produced at high titers in subtype C infections [103]. The fact that they are strain-specific suggests that they target the variable regions of *env.* Several studies have identified the V1V2 region as the most common target, followed by and the alpha-2 helix domain in the C3 region in subtype C infections [104 105]. The V4 and V5, are also targeted but to a lesser extent [104 106].

Because ssnAbs develop after viremia has peaked and target highly variable epitopes of Envelope, their activity is limited to viral variants that elicited their production, i.e. viruses circulating at a time preceding their development. They are therefore

ineffective against the currently circulating virus (contemporaneous viral variants) due to the rapid rate of viral escape, which is mediated by single or multiple mutations in the envelope. These mutations work by either sterically inhibiting antibody access to the epitope, or by directly changing the epitope so that it is no longer recognizable by the antibody. The most well documented mutations are the insertions/deletions (indels) that occur in the hypervariable regions. These indels typically alter the structure of the loops, which then masks the epitopes that would be targeted by neutralizing antibodies. Shifts in the glycan shield is also a common pathway to escape from nAbs.

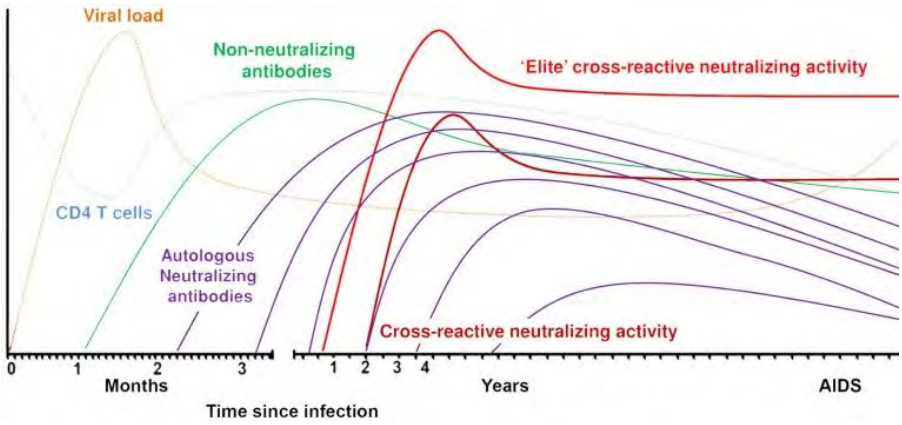

Figure 1.5. Evolution of antibody responses in HIV-1 infection over time. The first detectable antibodies are non-neutralizing and appear within days to one month following infection. Strain-specific, also known as autologous neutralizing antibodies emerge around two months post infection and may continue to appear all the way into chronic infection and disappear as infection proceeds to the AIDS state. Cross-reactive neutralizing antibodies and elite cross-reactive neutralizing antibodies appear between one and two years after. Elite cross-reactive neutralizing antibodies develop at about the same time as cross-reactive neutralizing antibodies and are also maintained into the AIDS state (Figure from Euler. & Schuitemaker [107]).

Due to the ability of the virus to evade the ssnAb response, ssnAbs are considered an ineffective immune response. However , some studies have shown that ssnAb can limit HIV-1 replication in early infection [108] [109] [110] [111]. CAP88 – a participant in the CAPRISA 002 cohort – had viral loads that declined when ssnAbs were able to neutralize 50% of the viral population and continued to decline as neutralization titers increased [108]. However, viral load rebounded upon the first detection of mutations in the viral *env* that rendered the viruses resistant to neutralization by ssnAb (**Figure 1.6**). Thus demonstrating that control by ssnAbs is transient due to rapid immune escape.

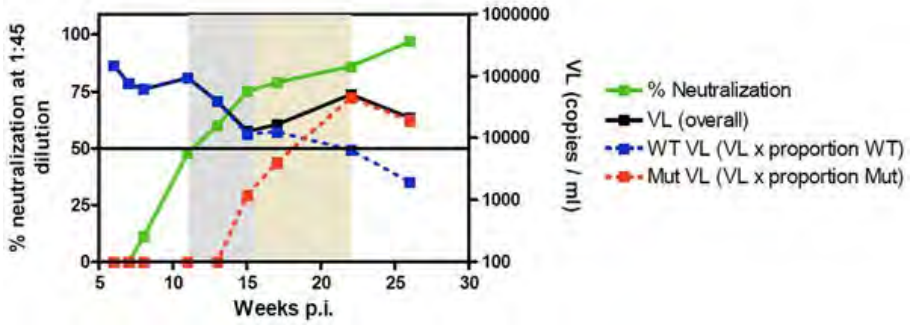

Figure 1.6. Neutralization escape following development of the mutant viral variants. Percent neutralization is shown as a green line, the viral load as black, wildtype viral load (WT VL) as blue and mutant viral load (Mut VL) as red. WT VL (blue line) declined between 11 and 15 weeks post infection (the gray-shaded area) and coincided with the increase in neutralization percentage (green line). At about 15 weeks p.i., The mutant viral load (MT VL, red line) emerged at 15 weeks post infection, resulting in the rebound of the overall viral load (VL, black line), and further decline in the WT VL in the area shaded brown (Figure from Moore *et al*. [108]).

1.7.2.4 Broadly cross-neutralizing antibodies

Broadly cross-reactive neutralizing antibodies (bnAbs) are antibodies that are able to neutralize a wide range of HIV-1 variants, including viruses from different subtypes. The ability to neutralize a broad range of viruses is known as 'breadth'. It has recently been shown that about 50% of HIV-1+ people had sera that could neutralize 50% of the viruses in the panel used [112] whilst some bnAbs are able to neutralize more than 80% of viruses. Generally, they develop between one and three years post infection in 20 to 30% of infected individuals [113] [114].

The recent discovery of monoclonal antibodies with exceptional breadth has enabled the detailed elucidation of bnAb targets. There are five classes of bnAbs characterized by the regions of envelope they target. The most common class of bnAbs is those that target the V1V2 regions targeted by PG9/16-like antibodies, as is the case for the ssnAb targets. Other targeted regions are: the glycan-dependent epitope in the C3 region targeted by PGT128-like antibodies; the CD4 binding site targeted by VRC01-like antibodies; and the membrane-proximal region (MPER) targeted by 4E10-like antibodies. Recently, another bnAbs epitope has been identified at the interface of gp120 and gp41, targeted by the monoclonal antibody 8ANC195) (**Figure 1.7**) [115] [116] [117] [118] [119] [120] [121].

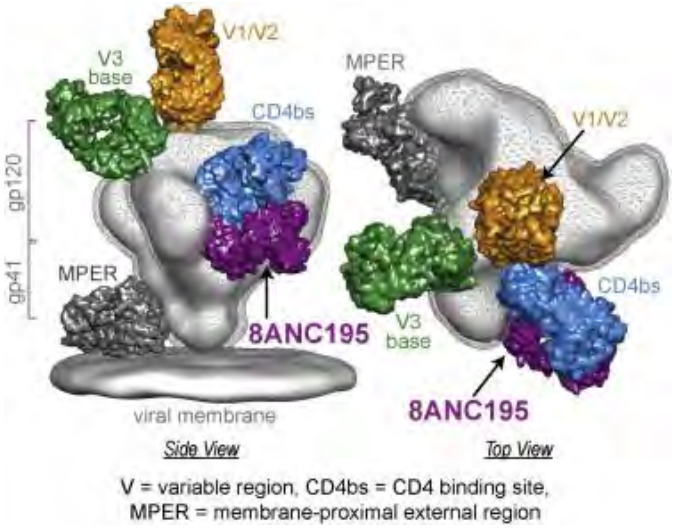

Figure 1.7. Broadly neutralizing antibody targets. Side and Top view of the HIV-1 spike made up of gp120 and gp41 (gray). The broadly neutralizing antibody targets are shown in various colours: V1V2 (yellow), CD4 binding site (CD4bs, blue), MPER in dark gray, the glycan-dependent V3 epitope in green and lastly the epitope at the interface of gp120 and gp41 shown in purple. 8ANC195 is shown here as a representative of antibodies targeting this interface (Figure from Scharf *et al.* [121]).

In addition to other immune response (e.g. cytotoxic T cell response), an effective vaccine would likely need to induce broadly neutralizing antibodies. Although they do not have clinical benefit to the individuals in whom they develop [122], bnAbs are shown to have therapeutic benefits in humanized mice and nonhuman primates in several studies. These studies show that administration of monoclonal bnAbs alone or in combination into SHIV-infected nonhuman primates or HIV-1 infected humanized mice reduced viral loads to undetectable levels [123] [124] [125]. SHIV (a chimeric HIV and SIV virus) acquisition was also prevented in macaques who received passive transfer of monoclonal antibody before being challenged with SHIV [125] [126]. Caskey et al. (2015) conducted the first human study where a monoclonal antibody, 3BNC117, was

administered in HIV-1+ and HIV-1- individuals [127]. The study does not show whether or not infection was prevented in the negative individuals, but they do show that viral load was suppressed in the infected individuals who received several doses of the 3BNC117 monoclonal antibodies.

1.7.2.4.1 Characteristics of broadly neutralizing antibodies

The studies above highlight the importance of the broadly neutralizing antibody responses in HIV-1 prevention and therapy. The ability to induce bnAb before HIV-1 exposure has the potential to protect against infection in humans, as seen in nonhuman primates. However, these antibodies have complex characteristics and maturation pathways, which contribute to the difficultly of designing an immunogen that would elicit these antibodies through vaccination. In addition, these characteristics vary according to the class of bnAb: The CD4-binding antibody class typically shows a high somatic mutation rate in the antibody heavy chain complementarity determining regions 2 (HCDR2) [128]. This allows for an interaction between the antibody and the epitope that mimics CD4 binding [129] [130] [131]. The antibodies that recognize the glycan-dependent epitopes in the V1V2 class have comparatively long HCDR3 loops, with high rates of somatic mutation. This length of the HCDR3 loops allows penetration of the glycan shield and access to the epitope. The MPER and N332 glycan in C3 classes also have long HCDR3 and high levels of somatic mutation [132].

It is clear that bnAb classes have unique features that separate them from other neutralizing antibodies. A vaccine aiming to elicit one or more of these antibodies may need to recapitulate the developmental pathway to induce the same characteristics described above.

1.7.2.4.2 Developmental pathway of broadly neutralizing antibodies

To understand how bnAbs develop, it is important to consider the events that occurred prior to their development, i.e. the interactive evolution of the strain-specific response and the transmitted virus. Two separate studies, Liao *et al*. [133] and Doria-Rose *et al*. [134] showed that strain-specific neutralizing antibodies drove early viral escape, which in turn facilitated the diversification of an antibody lineage towards the development of breadth bnAb.

In the Liao *et al*. study [133], donor CH505 was followed from acute infection to more than 3 years post infection – that is after development of the bnAb response. CH103, the antibody lineage that conferred broad neutralization, targeted the CD4 binding site. The emergence of the CH103 germline was dated to 4 weeks post infection (w.p.i), whilst the bnAb response emerged between 42 and 92 w.p.i. The earliest mutations in *env* coincided with the development of the first neutralizing antibodies. The t/f virus bound well to the antibody germline sequence known as the unmutated common ancestor (UCA), but heterologous envelope proteins could not bind UCA. This suggested that the antibody-binding was highly strain-specific. Conversely, late intermediate antibodies of this antibody lineage could not bind to transmitted virus, but could bind heterologous Env, suggesting that these antibodies had undergone somatic hypermutation to allow neutralization of the evolved Env.

In the Doria-Rose et al study [134], the development of bnAbs was investigated in participant CAP256 of the CAPRISA002 cohort. This donor was initially infected with one virus, and superinfected with a second strain 15 weeks later. In this individual, the CAP256-VRC26 bnAb clonal lineage targeted the V1V2 region. Their data showed

that the CAP256-VRC26 antibody lineage neutralized the superinfecting virus, but not the primary infecting virus. This suggested that the superinfecting virus primed the initial B cell response. Mutations in *env* were detected in the superinfecting virus at the time of the emergence of the first CAP256-VRC26 antibody response, suggesting the antibody responses drove escape in the superinfecting virus [135].

What these two studies show is that strain-specific neutralizing antibodies target a very narrow range of envelope variants. The development of this response drives viral diversification in the targeted epitope towards viral variants that are resistant to neutralization. Neutralizing antibodies, primed by the founder virus, undergo affinity maturation which, in some cases, leads to antibody daughter lineages that are better able neutralize a broader range of viral variants (**Figure 1.8**). To facilitate vaccine designs that will induce bnAb responses, it is important to understand the relationship between ssnAbs and viral evolution in the development of bnAbs.

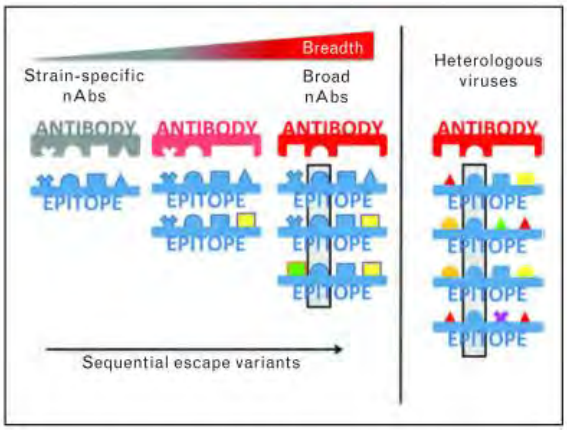

Figure 1.8. Development of broadly neutralizing antibodies from strain-specific neutralizing antibodies. Strain-specific neutralizing antibodies target single epitope. The epitope evolves by accumulation of mutations, resulting in various escape viral variants. At the same time, the antibody undergoes evolution. Escape variants and neutralization breadth increase over time (Figure from Derdeyn, Moore & Morris [154]).

Aim

To characterize the early strain-specific neutralizing antibody response; and resulting viral evolution; and to determine the relationship between epitopes targeted between strain specific neutralizing antibody and the later broad neutralizing response in an individual who subsequently developed broadly cross-neutralizing antibodies.

Rationale: The complex characteristics of broadly neutralizing antibodies suggest that it will be difficult to elicit these responses by vaccination. One school of thought is that viral evolution drives the development of breadth, and that this could be recapitulated in humans through sequential vaccination with viral variants responsible for eliciting breadth [136] [133137] [138] [134]. This project will characterize viral variants and strain-specific and broadly neutralizing antibody targets in early infection in CAP292, a participant of the CAPRISA004 trial, who developed neutralization breadth at one year post infection. The project forms part of a larger study that will define virus-host co-evolution over three years in CAP292 with the aim to define viral and host factors conducive to the development of BCN antibodies in natural infection. The overall purpose is to design cocktail vaccines that recapitulate epitope diversification in natural infection ("Broad Neutralizing HIV-1 Antibodies, Adjuvants and Immunogens", Principal Investigator P. Moore).

Objectives

- To determine the multiplicty of infection and identify the transmitted founder virus(es)
- To determine the kinetics of the early strain specific neutralizing antibody responses in a broad neutralizer, CAP292.
- To identify sites under selection pressure from strain-specific neutralizing antibodies and to map the targets for the early neutralizing response.
- To screen a panel of well-characterised bnAb escape variants, to identify broadly neutralizing antibody specificities.

2 Methods and materials

2.1 Selection of study subject and plasma samples

CAP292, a participant from the CAPRISA (Centre for AIDS Program of Research in South Africa) 004 cohort, was selected for this study. The CAPRISA004 cohort was established for a trial to determine the effectiveness of a tenofovir microbicide gel in preventing HIV-1 infection in women [13]. HIV-1 infection date was determined as the midpoint between the last antibody-negative test and the first antibody-positive test, based on two HIV-1 rapid antibody tests (namely, 'Determine HIV1/2' [Abbot Laboratories, Illinois, USA] and 'UniGold Recombigen® HIV test']. HIV diagnosis was confirmed by RNA PCR and laboratory enzyme linked immunosorbent assay (ELISA). Following diagnosis, the CD4+ T cell count and viral load were determined using the TruCOUNT method (BD Biosciences, San Jose, USA) [139].

Plasma samples were collected weekly for 3 weeks, biweekly for 3 months and quarterly thereafter. Plasma samples for this study were selected from several time points spanning the first year of infection (6, 30, 58 w.p.i), as well as a three year time point (186 weeks post infection). These samples were made available by CAPRISA (Doris Duke Medical Research Institute, Nelson R Mandela School of Medicine, and University of KwaZulu-Natal). This study was approved by the University of Cape Town Research Ethics Committee (HREC 049/2014)

2.2 Extraction of viral RNA

HIV-1 RNA was extracted using the QIAGEN QIAamp ® Viral RNA Mini Kit (Qiagen, Valencia, CA) following the manufacturer's instruction. This method is based on pH and chaotropic salt dependent binding of nucleic acids to silica beads. Briefly, RNA was extracted from 140-200 µl plasma (for high and low viral load, respectively). Samples with less than 100 000 viral copies/ml were considered as low viral load when determining plasma volume for extraction. The extracted RNA was eluted in 50 µl AVE Elution buffer.

2.3 Synthesis of complementary DNA (cDNA)

The synthesis of the complementary DNA (cDNA) was carried using the SuperScript™ III Reverse Transcriptase System (Invitrogen Life Technologies, Carlsbad, CA) according to the manufacturer's instructions, using 50 µl RNA, 0.25 µM Oligo-dT primer (Invitrogen) and 0.5 mM of each dNTP (Invitrogen), made up to 65 µl with DEPC-treated water (Sigma-Aldrich, St Louis, MO). This mixture was heated at 65 ºC for 5 minutes to denature RNA secondary structure and allow primer binding. To this reaction, the second reaction mix containing 10 units of Superscript III Reverse Transcriptase, 1X First strand buffer, 5 mM of Dithiothreitol (DTT) (Invitrogen) and 2 mM RNaseOUT (Invitrogen), made up to 35 µl with DEPC-treated water (Sigma-Aldrich) was added and the reaction incubated at 45 ºC for 2 hours, followed by enzyme inactivation at 70 ºC for 15 min. RNA was removed from the sample, to prevent RNA from interfering with subsequent amplification steps, by the addition of RNase H (1 Unit) and incubated at 37 ºC for 20 min. The synthesized cDNA was stored at -20 ºC.

2.4 Single genome amplification of HIV-1 gp160

Single genome amplification (SGA) allows PCR amplification from a single DNA template molecule [61]. Given the diversity of HIV-1 quasispecies in samples at any given time, this precludes Taq induced errors such as recombination, which occurs when Taq switches from one template to one that is genetically different. Moreover, it reduces the chance of sample bias where re-amplification of one template is favoured. After amplification, a yield of less than 30% positive reactions indicates that amplification is highly likely to have occurred from one template in 80% of these positive reactions [61]. This method allows accurate molecular characterization of circulating viral strains.

Here, SGA of HIV-1 gp160 was done as nested PCR, with amplifications carried out in a 96 well PCR plate (WhiteHead Scientific). The first round PCR reaction contained 1X Platinum® Taq High-Fidelity polymerase buffer (Invitrogen), 2 mM MgSO4, 0.2 mM of each dNTP (Invitrogen), 0.2 µM Vif1 primer (5'-GGGTTTATTACAGGGACAGCAGAG -3'; HXB2 nt 4900 - 4923), 0.2 µM OFM19 primer (5'-GCACTCAAGGCAAGCTTTATTGAGGCTTA -3'; HXB2 nt 9604-9632) (WhiteHead Scientific; Appendix A), 0.025 units Platinum® Taq High Fidelity polymerase (Invitrogen) and 1 µl of the cDNA, made up to 20 µl with distilled H_2O. The cycling conditions were set at: 94 ºC for 2min, 35 cycles of 94 ºC for 15 seconds (s), 58 ºC for 30 s, and 68ºC for 4 min and a final extension step of 68 ºC for 10 min. The nested PCR was carried out as above with the following exceptions: first round PCR product (1µl) was used as the template and 0.2 µM of primers ENV1A-Rx (5'-CACCGGCTTAGGCATCTCCTATAGCAGGAAGAA-3') and EnvN (5'-

TTGCCAATCAAGGAAGTAGCCTTGTGT -3') were used, while the number of cycles was increased to 45.

2.5 Generation of chimeras using the overlap extension PCR and mega primer PCR strategies

HIV-1 Env chimeras were generated by introduction of the V1V2 and C3V4 regions from CAP292 into the neutralization resistant Env backbone from CAP239, for mapping of the strain-specific neutralizing antibody response. To map regions involved in escape at different time points, the V1V2 and C3V4 regions of the CAP292 t/f virus were introduced into the envelope of viruses from 30 and 58 w.p.i. These chimeras were generated using two strategies: overlap extension PCR [140] and the modified version of the overlap extension PCR [141], here referred to as the 'mega primer' strategy.

2.5.1 Primer design and chimera generation using the overlap extension PCR strategy

Env was amplified as three separate fragments; F1, F2 and F3 (which were complementary at the 3'-ends), in a 5-step PCR method. The F2 region was the region of interest. The amplification required six primers, including the forward primer EnvA (5'-GGCTTAGGCATCTCCTATGGCAGGAAGAA-3') and reverse primer EnvM (5'-TAGCCCTTCCAGTCCCCCCTTTTCTTTTA-3') [142] which bind at the start and at the end of *env*, respectively. The remainder of the primers were designed as follows:

EnvA was used as a forward primer for the amplification of F1. The reverse primer for F1 was designed to bind just upstream of the region of interest (F2) and had a ten base pair overlap with the forward primer for the amplification of F2. The reverse primer for F2 was designed to bind to the 3' terminal section of the region of interest, with a 5' overlap with the F3 forward primer. The F3 forward primer was designed to bind at the end of F2. EnvM was used at the F3 reverse primer, and bound to the 3' end of envelope gene (**Figure 2.1)**. To join the F1 and F2 fragments, the F1 and F2 PCR products were pooled. Due to the introduced sequence overlap between the terminal regions of the two fragments, the forward strands from each fragment will prime an extension, merging it with the corresponding strand from the other fragment. These were then amplified in the same reaction, using the EnvA and F2 reverse primers to make an F1F2 amplicon. Similarly, the EnvA and EnvM were used to link the F1F2 fragment to F3, thus generating a full length chimeric *env* sequence**.**

The primers were named according to the targeted region of envelope (V1V2 or C3V4); which fragment they amplify (F1, F2 or F3) and lastly, the primer orientation (forward or reverse) (Appendix A). The GC content and Tm of all primers were calculated using an online tool called IDT OligoAnalyzer (http://eu.idtdna.com/calc/analyzer), to ensure that primer binding would occur at a consistent temperature, for all of the various primer combinations.

PCR amplification was carried out in 50 ul reactions containing 1X Phusion Buffer, 0.2 mM dNTP, 0.25 mM of primers and 1 unit of Phusion enzyme. The cycling conditions were set at 94 ^{0}C for 3 min, 45 cycles of 94 ^{0}C for 30 s; various melting temperatures for the different primer sets for 30 s; 72 ^{0}C for 4 min, and final extension at 72 ^{0}C for 10 min.

Figure 2.1. Overlap extension PCR strategy. A Fragment 2 is amplified from a neutralization sensitive *envelope* backbone using F2 forward (F2.for) and reverse (rev) primers. The 5'-end of the F2 for primer is complementary to the 5'-end of the F1.rev primer. While the 5'-end of the F2.rev primer is complementary to the 5'-end of the F3.for primer**. B.** Fragments 1 and 3 are amplified from the resistant *envelope* backbone. Fragment 1 is amplified using EnvA is the forward primer and F1.rev as the reverse. Fragment 3, on the other hand, is amplified using F3.for as the forward and EnvM as the reverse**. C.** Fragments 1 and 2 are linked together by the complementary regions introduced by the primers. Primers EnvA and F2.rev are used to join the two fragments together to form one fragment**. D** A complete envelope chimera is formed by joining the fragment from **C** with fragment 3 using the EnvA and EnvM primers.

The construction of expression plasmids containing the chimeric envelopes was carried out as per section 2.11, followed by transformation into competent Top 10 *E-coli* cells (see section 2.12).

2.5.2 Primer design and chimera generation using the mega primer strategy

The mega-primer approach uses two primers in a two-step PCR method [141]. These primers were the forward and reverse primers used to amplify (F2) in the overlapping PCR approach. The 5'-ends of the primers were complementary to the sequences of envelope plasmid at the beginning and end of the region for which the chimera is being generated.

In the first PCR step, F2 was amplified as in the overlap extension PCR strategy. This amplicon was then gel extracted and purified, as described in section 2.7. Generation of a chimeric HIV-1 envelope plasmid (step two) was done using similar PCR conditions as above, with the following exceptions: 100 ng of F2 was used as a 'mega primer' and 50ng of the neutralization resistant *env* expression plasmid as a template. The extension time was increased to 10 min, as the entire plasmid is amplified during this protocol.

The amplification occurs when each strand of F2 acts as a mega primer on the respective strands of the template plasmid. After the first cycle, hybrid plasmids are produced, containing one parental template strand and one newly synthesized strand containing the introduced chimeric sequence (namely, the mega primer). From the second cycle onwards, both hybrid plasmids and fully chimeric plasmids are produced. The sample was then treated with 1 Unit of *DpnI* for 15 min to remove the original methylated *env* template (**Figure 2.2**). The chimeric envelope plasmid was then transformed into competent Top 10 *E.coli* cells as described in 2.12 and purified as in section 2.18. Successful generation of chimeric sequences was confirmed by Sanger sequencing (section 2.8)

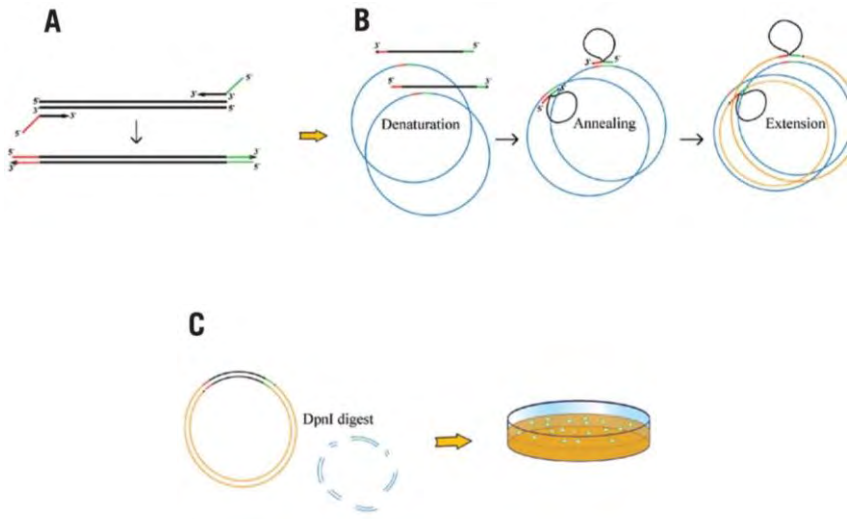

Figure 2.2. Mega primer chimera generation strategy. A. The region of interest (Fragment 2) is amplified using the designed primers. These primers are complementary to the corresponding regions on the plasmid**. B** The amplicon from **'A'** acts as a mega primer in the second reaction and plasmid as the template. The template is denatured, the mega primer anneals to the plasmid by complementarity, and extension is initiated from the primer 3'-end. Extension proceeds following the rolling circle mechanism until the 5'- end is reached. The mega primer replaces the corresponding region in the plasmid, forming the chimeric plasmid**. C.** The parental plasmid is degraded by *DpnI* digestion. The chimeric envelope plasmid is then transformed into competent cells [141]

2.6 Gel electrophoresis of PCR products

PCR products were electrophoresed on agarose gels (0.8, 1 or 2% (w/v) agarose in 1X TAE buffer (40 mM Tris base, acetic acid and 1 mM EDTA pH 8). PCR products were prepared with 1X loading dye (0.25 (w/v) bromophenol blue, 30% (v/v) glycerol, 0.25% (w/v) xylene cyanol FF,10X Gel Red) and electrophoresed at 100 V for 20 min in 1X TAE buffer. Amplified DNA was visualized under UV light using a UVITEC UVIPro Silver Gel doc machine.

2.7 DNA purification from agarose gel

DNA was purified from agarose gels using the crystal violet method (Invitrogen, Life Technologies). To prepare the gel, 40 ul of crystal violet was added to 50 ml 0.8% agarose gel, prepared as above. Electrophoresis was carried out at 100 V for 30 min and the gel was visualized under white light. Appropriately sized DNA fragments (~3 kb) were excised from the crystal violet gel and purified using the Zymoclean™ Gel DNA Recovery Kit (Zymoresearch, Irvine, CA), following the manufacturer's instructions. The purified fragments were eluted in 10 µl DNA Elution Buffer and DNA concentrations determined using a Nanodrop ND-1000 Spectrophotometer.

2.8 Sequencing of HIV-1 envelope clones and chimeras

Sanger sequencing of amplified DNA was performed at the Central Analytic Facility at the University of Stellenbosch, South Africa, on an ABI300 DNA Analyzer; using BigDye Terminator chemistry (Applied BioSystems, Foster City, CA). HIV-1 gp160 envelopes were sequenced using 12 overlapping primers (Appendix A).

2.9 Sequence assembly and analysis.

Sequences were edited and assembled in Sequencher® version 5.1 (Gene Codes, Ann Arbor, MI) to make full length envelope gp160 sequences. Firstly, the chromatograms were inspected for ambiguous base calls (double peaks). To qualify as an SGA sequence, all sequences that contain more than two double peaks were excluded from the analysis, as this indicates amplification from multiple templates. The resulting SGA sequences were aligned using Clustal W, and a consensus sequence generated in Bioedit version 7 [143]. Two online tools, one for generating a highlighter plot, showing sequence changes over time, (http://www.hiv.lanl.gov/content/sequence/HIGHLIGHT/highlighter.html), and another for plotting the entropy over time, at each position in the sequence, http://www.hiv.lanl.gov/content/sequence/ENTROPY/entropy_two.html, were used to visualize sequence diversity. Poisson Fitter (http://www.hiv.lanl.gov/content/sequence/POISSON_FITTER/poisson_fitter.html) was used to determine whether the distribution of the distance scores for the sequences could be fitted to the Poisson distribution. The number of potential N-linked glycosylation (PNLG) sites was determined using the program N-glycosite

(http://www.hiv.lanl.gov/content/hiv-db/GLYCOSITE/glycosite.html). The length of the variable loops was determined using the Variable loop characterization tool on Lanl (http://www.hiv.lanl.gov/cgi-bin/VAR_REG_CHAR/var_reg_char).

2.10 Amplification of HIV-1 envelopes for cloning into a mammalian expression system

Nested PCR reactions were carried out on first round PCR products from the SGA reactions (described in section 2.4) using the high fidelity polymerase Phusion Hot-Start (New England Biolabs, Ipswich, MA, USA). Each reaction contained 1 µl of the first round PCR DNA product, 1 Unit Phusion Hot Start Enzyme (Biolabs), 0.2 mM of each dNTP, 0.2 µM EnvM reverse primer (5'–TTGCCAATCAGGGAAGTAGCCTTGTGT-3'), 0.2 µM Env1Arx forward primer, containing a 5' CACC overhang allowing directional cloning, (Env1Arx: 5' - CAC CGG CTT AGG CAT CTC CTA TAG CAG GAA GAA-3';) and made up to 50 µl with distilled H_2O. The cycling conditions were set at: 94 ºC for 5 min, 45 cycles of 94 ºC for 30 s, 55 ºC for 30 s, and 72 ºC for 5 min and a final extension step of 72 ºC for 10 min. Phusion reaction products were purified as per section 2.7.

2.11 Generation of an mammalian expression vector containing HIV-1 envelope

Pseudotyped Env expression vectors were prepared using the pcDNA™3.1/V5-His TOPO® TA Expression Kit (Invitrogen) according to the manufacturer's instruction. The ligation of the purified envelope with the pcDNA3.1/V5-His-TOPO plasmid (Invitrogen) occurs through the annealing of the 3'-A overhangs on the envelope,

introduced by the Phusion polymerase, to the 5'-T overhangs on the linearized plasmid. Ligation was performed in 6 µl reactions containing: 30 ng of envelope DNA, 10 ng of the pcDNA3.1/V5-His-TOPO plasmid and 1 µl salt solution, made up to 6 µl with sterile water. Reactions were incubated at room temperature for 5 min.

2.12 Transformation of Top10 competent *Escherichia coli (E. coli)*

Top10 competent *Escherichia coli (E. coli)* cells (Invitrogen) were used for the transformation of *env*-containing pcDNA3.1/V5-His-TOPO plasmid, using the heat shock transformation method specified in the pcDNA™3.1/V5-His TOPO® TA Expression Kit. The ligated vector was incubated with the TOP 10 cells on ice for 30 min, followed by heat shocking at 42 ºC for 30 s. The transformed cells were incubated in Luria-Bertani Broth (LB) (1 % (w/v) Tryptone, 1% (w/v) yeast extract and 0.5% (w/v) Sodium Chloride) for 1 hour at 32 ºC, to express the ampillic resistance gene, following which they were plated out on luria agar (0.5% (w/v) peptone, 0.25% (w/v) yeast extract ,0.1% (w/v) glucose and 1.5% (w/v) agar) containing 100 mg/ml carbenicillin antibiotic and incubated overnight at 32 °C.

2.13 Screening of colonies for successful transformation

Colony PCR (cPCR) was used to screen the transformants for successful cloning of *env* into the pcDNA3.1/V5-His-TOPO plasmid. The cPCR reaction mix contained: 0.25X Superrtherm Taq Buffer, 1 mM MgCl2, 0.25 mM dNTPs, 2 µM T7 forward primer (5´TAATACGACTCACTATAGGG-3'), 2 µM BGH reverse primer

(5´TAGAAGGCACAGTCGAGG-3') and 0.0375 Units Supertherm Taq Polymerase. The cycling conditions were set at: 94 ºC for 30 s, 35 cycles of 94 ºC for 30 s, 51 ºC for 30 s, and 72 ºC for 3 min and a final extension step of 72 ºC for 10 min. Products was separated on 1% (w/v) agarose gel and viewed under UV light. The presence of a 100 bp fragment was used to identify positive colonies.

2.14 Large scale plasmid preparation

Colonies, identified as positive by colony PCR, were inoculated into 5 ml of LB with 100 mg/ml of carbenicillin and incubated for 6 hours at 32 ºC. This starter culture was then transferred to a 1L flask containing 100 ml LB and 100 mg/ml carbenicillin and incubated overnight at 32 ºC. The *env*-containing pcDNA 3.1/V5-His TOPO plasmid was prepared from 50 ml of overnight culture using the QiAprep spin Miniprep kit (Qiagen) following the manufacturer's instructions. The plasmid DNA was eluted in 50 µl sterile water and the concentration determined using a NanoDrop. DNA was stored at -20 ^{0}C, until use.

2.15 Cell line maintenance and preparation

Cell lines of adherent TZM-bl and HEK293T cells were maintained in T75 flasks containing complete growth medium (GM) (Dulbecco's Modified Eagle Meduim (DMEM) with L-glutamine, sodium pyruvate, glucose and pyridoxine (Gibco BRL Life Technologies), 10% Fetal Bovine Serum (FBS) heat inactivated at 56 ºC for 1 hour, 10 mM HEPES (N-2-Hydroxyethylpiperazine-N'-2-Ethanesulfonic Acid) (Gibco BRL Life Technologies), 50 µg/ml Gentamicin solution (Sigma-Aldrich). Cells were incubated at

37 ºC, with 5% CO_2 and 90% humidity until confluent, usually 2-3 days. The monolayers were disrupted at confluency by treatment with Trypsin-EDTA (0.25% trypsin, 1 mM EDTA) (Invitrogen) as follows: Growth medium was removed from the flask. The monolayers were washed with 5 ml Phosphate Buffer Saline (PBS, without magnesium or calcium), to remove residual serum. TZM-bl and HEK293T cells were then incubated with 2.5 ml and 1 ml 0.25% Trypsin-EDTA respectively, to disrupt adherence, following which, cells were incubated at room temperature for 5 min for TZM-bl and 1 min for HEK293T cells. Trypsin activity was disrupted by addition of 10 ml GM.

2.16 Cell counting

10 ul of trypsinized cells on GM were stained with 10 ul 0.4% Trypan Blue (Sigma-Aldrich) and counted using a hemocytometer, with cells counted in the four major quadrants. The total number of cells contained in 1 ml of the typsinized cell suspension was obtained by multiplying the number of cells counted by 5000 (dilution factor * 10 000 cells/ml).

2.17 Generation of pseudotyped viruses by transfection of HEK293T cells using molecular clones

Env-pseudoviruses were generated by co-transfection of an env-deficient plasmid, pSG3Δenv, and a vector containing a cloned *envelope,* i.e. *env*-pcDNA3.1/V5-His-TOPO plasmid, into HEK293 T cells. Three million HEK293T cells were grown overnight in T75 flasks under the following conditions: 5% CO_2, 90% humidity and 37

°C. The cells were transfected with 4 µg of *envelope*-pcDNA3.1/V5-His-TOPO and 8 µg of pSG3Δ*env*, using the polyfect transfection kit, according to the manufacturers instructions (PolyFect® Transfection Reagent Handbook, September, 2000). Briefly, non-phenol red DMEM (Gibco, Life Technologies, Carlsbad, CA) was added to the DNA, following which 40 µl Polyfect Transfection Reagent (Qiagen) was added and the transfection mixture incubated at room temperature for 10 min. Polyfect allows formation of DNA complexes that facilitate efficient transfection. Complete GM was slowly added to the mix, which was transferred to the T75 flask of the HEK293T cell monolayer. Cells were incubated for 48 hours at 37 ºC and 5% CO_2 to express pseudovirus. Functional Env is produced from the pCDNA plasmid while additional components required for virion assemply are produced from the pSG3Δ*env* plasmid. This produces virus capable of only one infection cycle, which are thus termed pseudovirus. Pseudovirus-containing media was harvested after 48 hours and passed through a 0.45 µm filter to remove any cells. The serum concentration of the media was adjusted to 20% by addition of 100µl heat inactivated FBS and stored at -80 °C.

2.18 Titration of pseudovirus particles for neutralization assay ($TCID_{50}$ assay)

Pseudoviruses are called as such because of their inability to produce infectious virions due to the separation of the envelope from the other genomic regions. Thus, they can only undergo one cycle of replication, infectivity is detectable using an engineered cell line. TZM-bl cells are engineered to express high levels of CD4 and CCR5-receptors required for HIV-1 infection. Once the cells are infected, the viral transcription factor Tat initiates HIV-1 replication, This results in the expression of HIV-1 genes, as well as a luciferase reporter gene which has been engineered into the TZM-bl cell line. To

quantify the infectivity dose, a luciferase substrate is added. This is cleaved by the luciferase enzyme, giving off luminiscence which is detected on a luminometer as Relative Light Units (RLU).

To determine the infectivity dose of the pseudoviruses generated above, the pseudovirus was diluted in GM in a 96 well plate, using a fourfold serial dilution, carried out in duplicate. TZM-bl cells (10,000 cells/100 µl) containing 25 µg DEAE-Dextran/ml were added per well. The pseudovirus was incubated with these cells for 48 hours at 37 ºC, 5% CO_2 and 90% humidity. The infectivity of the pseudovirus was inferred from the RLU which are produced as a result of the virus infecting the cells. The BrightGlo Luciferase assay was used to determine the RLU produced at each of the dilutions. To perform the assay, 100 µl of growth media was removed from the well of the plates containing the virus and cell mixture before adding 100 µl BrightGLo luciferase substrate. The luciferase enzyme in the BrightGlo mix reacts with the substrate to give off luminescence, which was detected on a Promega Glomax 96 microplate luminometer. The $TCID_{50}$ was taken as the pseudovirus dilution that gives at least 10 000 RLU.

2.19 Neutralization assay using pseudotyped viruses

The TZM-bl cell line expresses both the CD4 and CCR5 co-receptors required for HIV-1 infection. During infection, luciferase is expressed under the direction of a Tat-induced promoter (Tat is an HIV transcription factor). The amount of luciferase produced, directly correlates with the number of successful infections. The neutralization assay was performed using a single-round TZM-bl reporter assay in duplicate, in a 96-well plate format. Pseudovirus was incubated with eight threefold dilutions of antibody, containing heat inactivated plasma (incubated at 56 °C for one hour to remove complement activity which may interfere with the neutralizition assay) and incubated for at least 45 min at 37 °C, CO_2, 90% humidity. TZM-bl cells (10 000 cells per well in 100 µl growth medium) were added to the pseudovirus-plasma mixture and incubated for 48 hours at 37 °C, CO_2 and 90% humidity. After 48 hours, the TZM-bl cells was lysed and evaluated for luciferase activity. The percentage infectivity was calculated using the macro luminescence sheet (available from www.hiv.lanl.gov). This sheet calculates the percentage neutralization for each of the plasma dilutions. The neutralization titers are then calculated as the reciprocal of the dilution that gives 50% neutralization.

3 Results

The design of immunogens that can elicit broadly neutralizing responses remains a priority in HIV-1 vaccine research. There is evidence that HIV-1 diversification may contribute to the development of broadly cross neutralizing antibodies. Recent studies in two individuals showed that viral escape from antibody pressure may have facilitated the maturation of the antibody response to develop breadth through the presentation of Env variants [133] [134]. Whether or not this pattern of concomitant viral evolution and antibody maturation leading to development of bnAbs can be generalized to other HIV-1 infected individuals is unknown. The aim of this thesis was characterise early ssnAb responses and the associated viral evolution in one individual from the CAPRISA004 cohort, and to determine the relationship between epitopes targeted by strain specific neutralizing and the broadly neutralizing antibodies.

3.1 Study participant

This study performed a detailed analysis of viral evolution in an HIV-1 in an infected woman, CAP292, who was in the placebo arm of the CAPRISA004 study that tested the effectiveness of a tenofovir microbicide gel in preventing HIV-1 infection in women [13]. CAP292 was infected in March 2008 and enrolled into the CAPRISA002 acute infection study in April of the same year. She developed some cross-neutralizing responses at 12 months post infection, and by three years post infection plasma from this participant neutralized 56% of viruses in a heterologous multi-clade panel of HIV-1 pseudoviruses (P. Moore, personal communication).

At enrolment into the cohort, CAP292 had a high viral load of 458 000 copies/ml, consistent with acute infection (**Figure 3.1**). The initial control of viral load to 34 700 copies/ml at 14 w.p.i was followed by a marked increase to 233 000 copies/ml by 30 w.p.i. The CD4+ T cell count was 510 cells/µl at enrolment and declined to 232 cells/µl by 21 w.p.i with the concomitant increase in viral load during this time period. Therapy was offered to all participants whose CD4 T cell count fell below 350 cells/µl, according the prevailing national guidelines. At this time CAP292 refused therapy (N. Garrett personal communication). By 186 w.p.i, the viral load declined to 32 000 copies/ml where the CD4 count was 392 cells/µl.

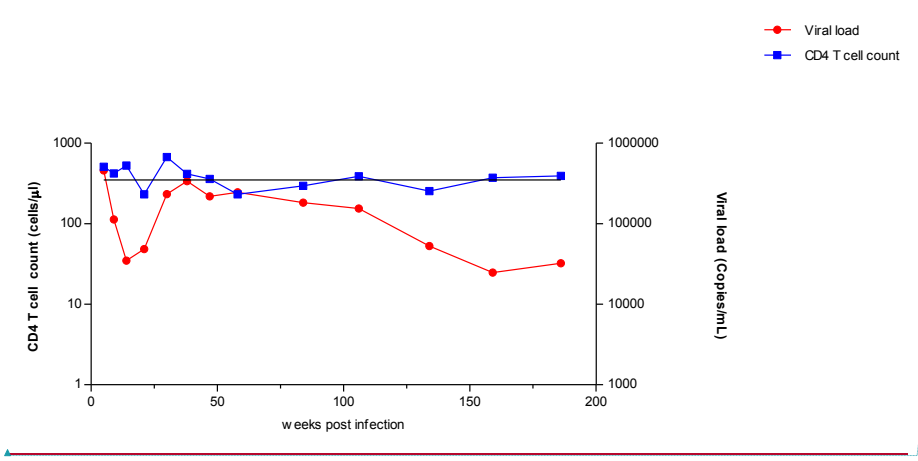

Field Code Changed

Figure 3.1. Viral load and CD4+ T cell trajectory in CAP292.
The black line at 350 cells/µl, represents the CD4 count threshold for initiation of ARV according to the prevailing National Guidelines.

3.2 The CAP292 transmitted/founder (t/f) virus envelope

To determine the kinetics of early ssnAb responses it was necessary to identify the *env* sequence of the virus that established the infection, the transmitted/founder (t/f). Due to rapid escape from nAbs, ideally this requires sampling prior to immune pressure, or at least prior to the development of nAb responses.

To identify the t/f *env* sequence in CAP292, SGA followed by sequencing was carried out [61]. To generate single genome amplicons, cDNA was diluted such that after amplification, there were less than 30% positive reactions, which according to the Poisson distribution, implies a high likelihood that amplification was from one template in more than 80% of positive reactions [61]. Whilst it was optimal to determine the t/f *env* at the closest time point to infection, amplification from the five w.p.i sample was unsuccessful despite repeated attempts at RNA extraction and re-amplification. It was suspected that the RNA from this sample had degraded, thus, RNA from the next available time point (6 w.p.i.) was used. The amplification of *env* from cDNA at a 1:81 dilution generated less than 30% of the positive amplification reactions (**Figure 3.2**).

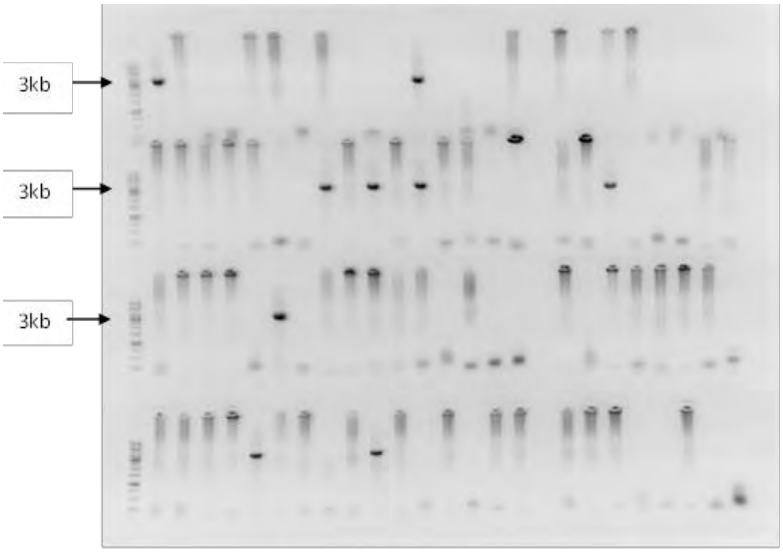

Figure 3.2. A representative for envelope single genome amplification (SGA) of CAP292 at 6 weeks post infection. The SGA amplicons were electrophoresed on a 1% agarose gel with a 1kb molecular weight marker (M) (Thermo Fischer Scientific, Waltham, MA, USA). Positive amplification is indicated by the presence of distinct DNA fragments at 3kb (indicated by arrows).

A total of 16 SGA sequences, which had no nucleotide ambiguities, were used in further analysis. We determine the multiplicity of infection based on criteria established by Keele and colleagues (2008) whereby an infection was identified as being founded by a single variant if it met the following criteria: no shared mutations in the population; low genetic diversity; Poisson distribution of hamming distances; and sequences conforming to a star-like phylogeny.

The sequences in CAP292 had very low diversity, with a mean genetic distance of 0.001 (range 0 to 0.003). A frequency plot of hamming distances, which computes a

pairwise measure of the number of base differences between sequences, shows a Poisson distribution consistent with single variant infection (**Figure 3.3**).

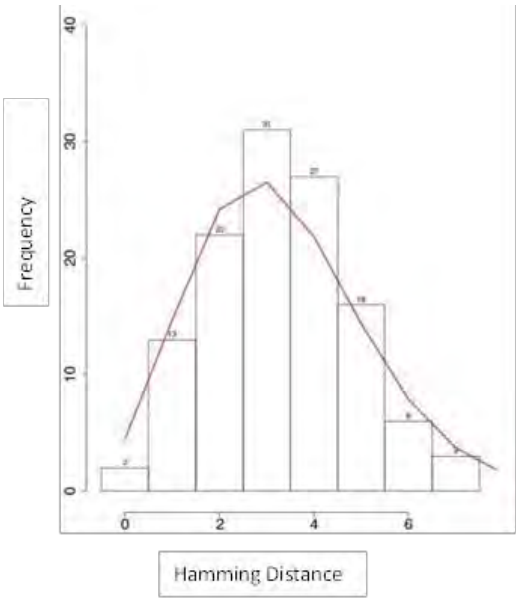

Figure 3.3. Hamming distance frequency distribution. The frequency was plotted as the number of sequences with the same hamming distance. The line of best fit is indicated in red. The hamming distances was plotted from an alignment of 16 SGA sequences from the 6 w.p.i time point. The length of the sequences was 2586 nucleotides.

The sequence phylogeny was assessed using a neighbour joining tree and the diversity analysed in the highlighter plot (**Figure 3.4**). The highlighter plot (www.hiv.lanl.gov/highlighter), 'highlights' the nucleotides which differ from the consensus sequence, in each sequence in a nucleotide alignment. The neighbour joining tree showed limited divergence, with two sequences: 1A_6w.p.i and 9H_6w.p.i being identical to the generated consensus sequence. The sequences 6D_6w.p.i, 8C_w.p.i, 1D_6w.p.i and 1E_6w.p.i formed one sub-lineage, whilst a second sub-

lineage consisted of the 10C and 3B_w.p.i sequences. The sequences that formed the first sub-lineage (6D, 8C, 1E 1D_6w.p.i) had a shared mutation at position 2191, and the sequences 1D_6w.p.i and 1E_6w.p.i had an additional shared mutation at position 1103. Similarly, in the other sub-lineage consisting of the sequences 10C and 3B_w.p.i, there was a shared mutation at position 1629. As this individual had been infected for approximately 6 weeks, we propose that the observed shared mutations between sequences was a result of mutations introduced and replicated in early infection, rather than infection with multiple variants.

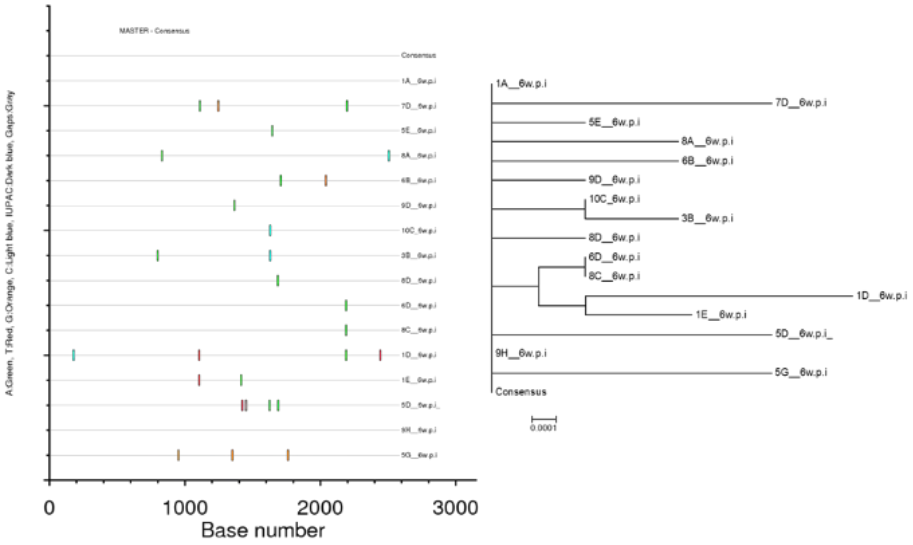

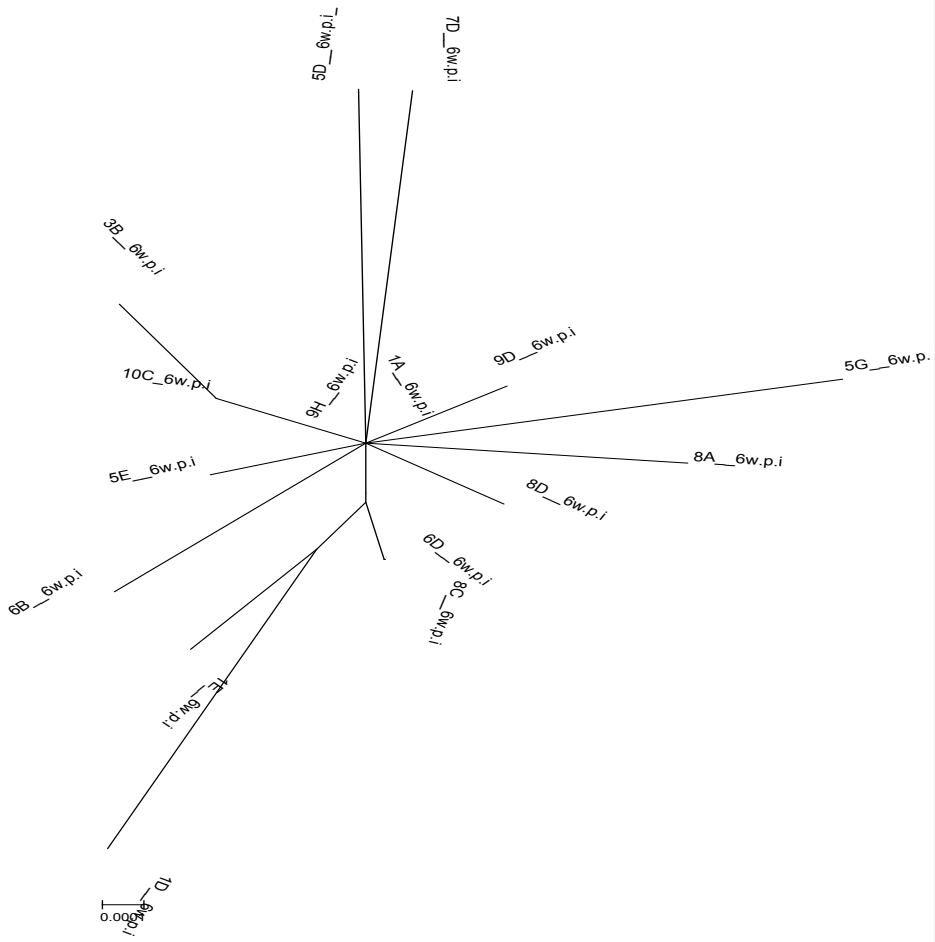

Figure 3.4. Analysis of CAP292 SGA sequences at 6 weeks post infection. The sequences are compared to the consensus (master sequence) in the nucleotide highlighter plot (left). Variations from the consensus are represented by the coloured stokes (key is shown on the left). The neighbour joining tree (middle), rooted at the consensus, and shows the phylogeny of the sequences. The distance scale bar is indicated. The star-like phylogeny of the sequences is shown on the left.

The distribution of the DNA distances fit the Poisson model (**Figure 3.3**), and this together with star-like phylogeny (**Figure 3.4**) and low diversity suggested infection by a single viral variant. There were two SGA sequences that matched the consensus exactly. One of these, sequence 1A_6w.p.i, was chosen as the representative of CAP292 t/f *env.*

3.3 Neutralization profile of the transmitted/founder (t/f) virus.

Strain-specific neutralizing antibodies (ssnAb) are the first neutralizing antibodies to develop against HIV-1 [144] . In order to determine the timing of development of ssnAb, the SGA sequence 1A_6w.p.i (identical to the consensus sequence) was cloned to generate the CAP292 t/f *env* pseudovirus. The clone was sequenced to confirm that no errors had been incorporated during the PCR and cloning steps. The CAP292 t/f *env* pseudovirus was subsequently tested against plasma spanning the first year of infection for neutralization sensitivity.

The first neutralizing antibody response was detected at 14 w.p.i, at low potency (ID_{50} of 1:92) (**Figure 3.5**). The antibody titers appear to track the increase in viral load rising to ID_{50} of 1:782 by 30 w.p.i and 1:1139 by 58 w.p.i, where viral load and neutralization titers stabilized. The concomitant increase in viral load with neutralization titer suggested that the strain-specific response had no impact on viral replication.

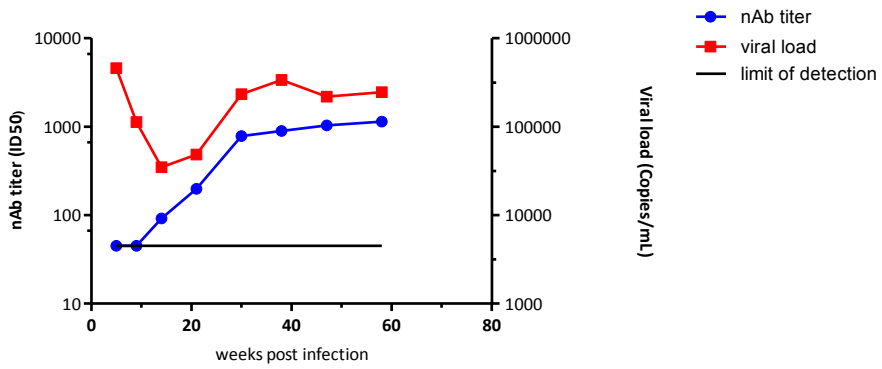

Figure 3.5. Neutralization kinetics of the transmitted/founder virus (blue line) and viral load (red line). The increase in viral load after peak viremia coincided with emergence of the first neutralizing antibodies at 14 w.p.i. The nAb titers increase steadily up to 58 w.p.i. The black line indicates the limit of detection for neutralization sensitivity (ID_{50} < 1:50).

3.4 Evolution in Envelope over three years

Neutralizing antibody responses drive viral escape, which is typically mediated by insertions and deletions, and shifts in potential N-linked glycan sites. A lowered net negative charge of Env has also been associated with resistance to neutralization [112], and there is evidence that the net charge of virus and antibody co-evolve over time [134]. To identify sites under antibody pressure, we examined the *env* viral sequences from longitudinal time points.

A total of 59 SGA sequences were generated from five time points: 6 w.p.i (prior to nAbs); 14 w.p.i (around the time of strain-specific nAbs developed; 30 w.p.i.; 58 w.p.i (at the time development of early neutralization breadth); and 186 w.p.i (peak neutralization breadth). An average of 11 SGA derived sequences were generated per time point, with the phylogenies illustrated in **Figure 3.6**. The sequences clustered

according to time post infection, except at 6 and 14 w.p.i, which made up a single cluster due to a low level of sequence diversity. The intermixing of the sequences from these two early time points suggested that there was limited selection between time of infection and at first detection of neutralizing antibodies at 14 weeks. The dramatic shift of the viral populations after 30 w.p.i. suggested strong selective pressure. The 6A_30w.p.i sequence did not cluster with the rest of the sequences at this time point. Instead this sequence appears to be the ancestor of the two clusters at 30 w.p.i and 58 w.p.i. Similarly at 58 w.p.i the sequences 4B_58w.p.i and 11C_58 w.p.i formed a cluster separate from the rest of the sequence at 58 w.p.i (**Figure 3.6**). The cluster at 158 w.p.i consisted of two distinct sub-lineages suggesting two separate escape pathways at this time point (**Figure 3.6).**

Figure 3.6~~3.6~~

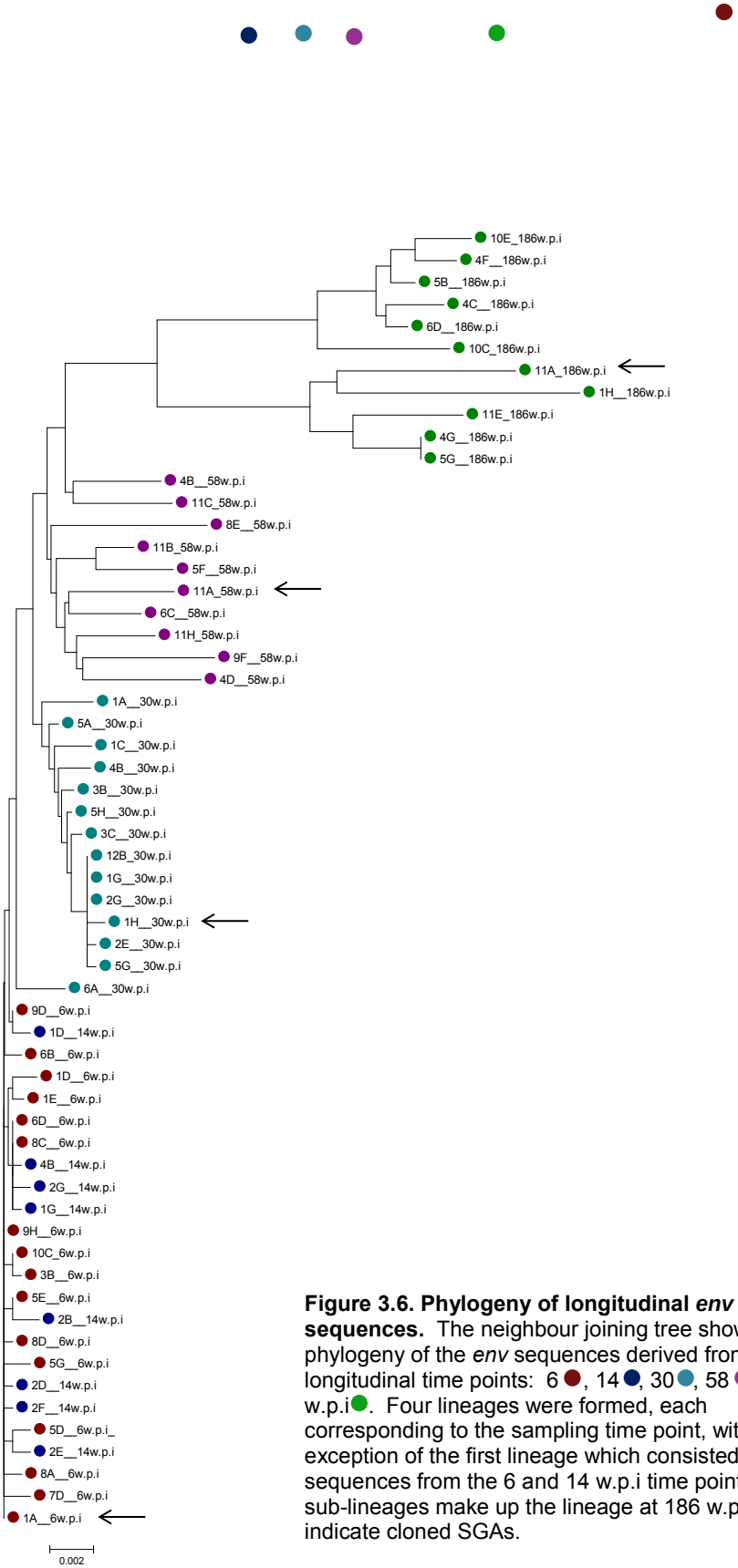

Figure 3.6. Phylogeny of longitudinal *env* sequences. The neighbour joining tree show the phylogeny of the *env* sequences derived from five longitudinal time points: 6 ●, 14 ●, 30 ●, 58 ●and 186 w.p.i●. Four lineages were formed, each corresponding to the sampling time point, with the exception of the first lineage which consisted of sequences from the 6 and 14 w.p.i time points. Two sub-lineages make up the lineage at 186 w.p.i. Arrows indicate cloned SGAs.

Divergence, defined as the average hamming distance (aHD) from the t/f *env* consensus sequence, increased gradually over time **(Figure 3.7).** The aHD at 6 w.p.i was 1.78, and increased to 52.14, 67.52 and 131.81 by 30, 58 and 186 w.p.i respectively. To estimate *env* variation within viral populations we calculated the standard deviation (SD) from the aHD at each time point. There was very little sequence diversity at 6 w.p.i (SD 1.7), indicating little selective pressure in early infection. After the development of nAbs at 30 w.p.i the diversity increased to SD 17, and interestingly was maintained at SD 18 at 58 w.p.i and at 186 w.p.i. Although the high diversity at the latter time points was expected due to the increase in antibody selective pressure, it was of interest that there was similar diversity at each time point from 30 weeks suggesting some selective pressure on viral populations constraining population diversity.

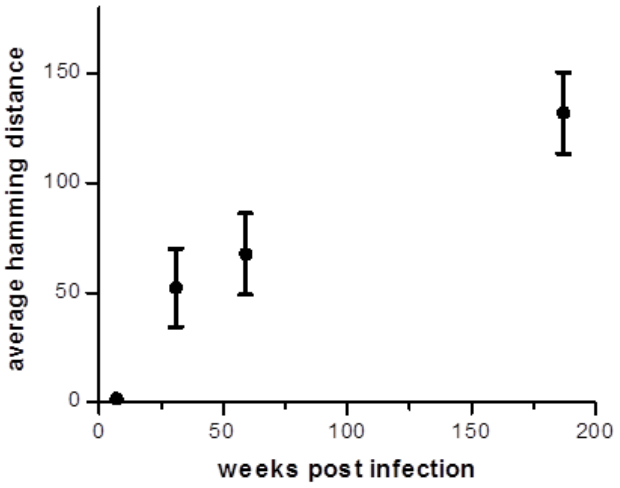

Figure 3.7. Divergence and diversity of sequences at sequential time points. Divergence was calculated as the average hamming distance (aHD) from the t/f sequences. The sequence diversity, calculated as the standard deviation (SD) of the average hamming distance, is represented by error bars.

3.5 Evolution in putative antibody sites

For identification of putative nAb escape mutations, the sequences were aligned to the t/f sequence and the variation from the t/f sequence was visualized on a highlighter plot (**Figure 3.8**). Putative immune escape was identified as shared mutations that became fixed over time. As escape is typically facilitated by changes in variable loop length, N-linked glycan sites and Env net charge, and elongation of the variable loops has been shown to confer resistance to neutralization [112], we also analysed changes in these properties over time.

The highlighter analysis shows very little sequence variation between the 6 and 14 w.p.i time points (**Figure 3.8**). The mutations that occurred during this time period were mostly scattered across envelope, suggesting random viral evolution which is consistent with a lack of strong antibody pressure. There was, however, a G459S shared mutation in the V5 region (**Figure 3.9**). This mutation was found in one sequence at 6 w.p.i, one at 14 w.p.i and in all but one of the sequences at 30 w.p.i but not at subsequent time points. Another shared mutation (E735K) was found at position in the intracellular domain of gp41 in 6/24 of the sequences at 6 and 14 w.p.i combined (**Figure 3.9**). Similar to the mutation in V5, the E735K mutation (all references are to HXB2 numbering) was not detected at any of the other time points. This data indicates selective pressure that acted on viral variants circulating before detection of the first neutralizing response, although these mutations may also have been introduced by chance.

The first persistent mutations were detected at 30 w.p.i, and occurred mostly in the gp120 region (**Figure 3.8**). Deletions were detected in the V1V2 region, while non-

synonymous changes were identified in multiple regions of envelope. The gp41 was particularly conserved, having only a few persistent nonsynonymous mutations at 30 w.p.i, however there were more nonsynonymous mutation in the gp41 at 186 w.p.i, after development of the broadly neutralizing response.

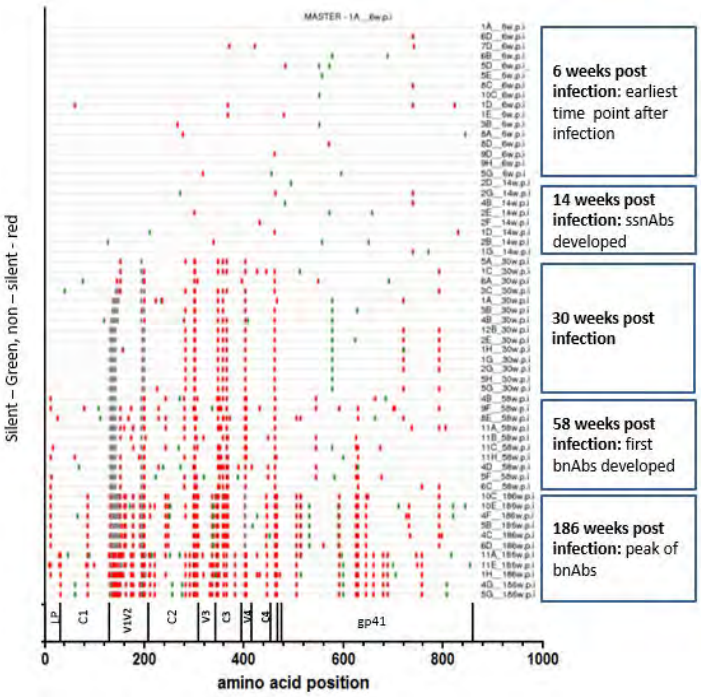

Figure 3.8. Synonymous/non-synonymous plot analysis of envelope SGA sequences over time. SGA sequences were generated from five sequential time points. All sequences are compared to the master sequence 1A_6 w.p.i t/f. Nonsynonymous, synonymous mutations and gaps are represented by green, red and gray respectively. The different regions of env are annotated below the plot, with LP indicating the Env leader sequence.

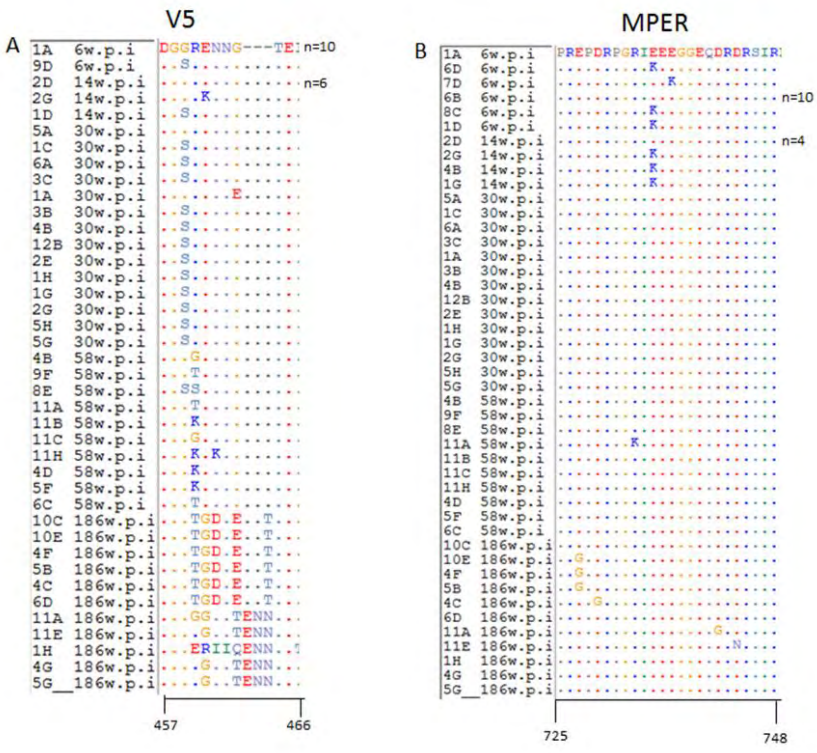

Figure 3.9. Evidence of early immune pressure in the V5 and intracellular domain of gp41. Amino acid alignment of the V5 region A, shows the G459S mutation in the sequences 9D_6w.p.i, 1D_14 w.p.i and in all but two sequences at 30 w.p.i. In gp41 B, an E735K mutation occurred in the intracellular domain in 6/24 sequences at 6- and 14w.p.i combined. HXB2 numbering was used. “n” indicates the number of sequences matching the clone next to which n appears.

Analysis of loop-length and shift or change in N-glycan site identified a marked shortening of the V1V2 loop from a median of 77 amino acids following transmission

to 62 amino acids at 186 w.p.i (**Figure 3.10A**). This was accompanied by a reduction in the number of potential N-linked glycan sites from eight to 6 between 6 and 186 w.p.i. The length of the V3, V4 and V5 regions was constant throughout infection. However, variation within these loops included an increase in the number of glycosylation sites, which tended to increase by one site by 186 w.p.i in the V3 and V4. The overall net charge was neutral by 186 w.p.i, from a charge of -2 in the t/f virus (**Figure 3.10B**). While the net charge was constant in the V3 region, in V4, the charge increased from +1 to +2 at 186 w.p.i. Inversely, the charge changed from -2 at transmission to -3 in the V5 by 186 w.p.i.

A

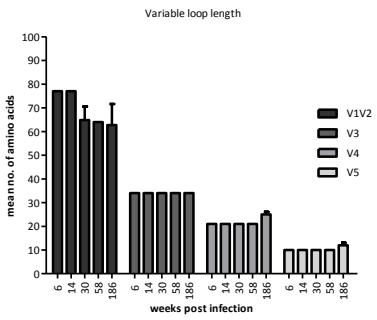

B

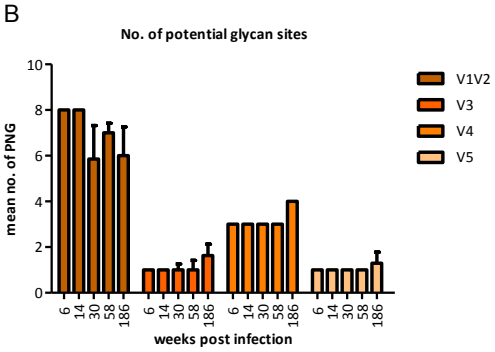

C

Average Net charge				
w.p.i	**V1V2**	**V3**	**V4**	**V5**
6	-2	4	-1	-2
14	-2	4	-1	-2
30	-1	4	-1	-2
58	-2	4	0	-2
186	0	4	1	-3

Figure 3.10. Variable loop region characterisation over time. **A**. Average variable loop length variation, **B**. average number of potential N-linked glycosylation sites and **C**. average net charge (red: negative, blue: positive, white: neutral charge). The error bars indicate the standard deviation in the variable loop length and number of potential N-linked glycan sites.

Together, these data showed that Env evolved through changes in the variable loop lengths, number of glycosylation sites and net charge. Most of these variation occurred in the V1V2 region suggesting that this regions largely contributed to the changes in the Env of successive viral populations.

Molecular characterisation of the V1V2 region (**Figure 3.11**) showed a deletion between positions 132 and 145, which was first introduced at 30 w.p.i and maintained until 58 w.p.i. This deletion resulted in the disruption of an N-linked glycosylation site at position 135.1 in the t/f virus, where 135 would be the HXB2 position and the decimal point representing insertions relative to the HXB2 number. At 186 w.p.i, the viral populations were split into two subpopulations: the first 6 sequences in the alignment at this time point (here forth referred to as sub-lineage 1) showed several distinct sequence changes from the other five sequences (sub-lineage 2), indicating that these two lineages may be the result of alternative escape pathways. In the sub-lineage 1 sequences, a deletion between 135 and 144 resulted in abrogation of two N-linked glycan sites at positions 135.9 and 141. Sub-lineage 2 had the T135.6N and G135.8T mutations that introduced an N-linked glycan site at position 136.6. An E169K charge change mutation was detected in sub-lineage 1, while sub-lineage 2 had an R170K mutation, maintaining the positive charge at this position. A substitution of N to T at position 135.1 shifted the N-linked glycan site from 135 to 133 in both the sub-lineages. The N-linked glycan site at position 186 was removed by the S189N at 30 w.p.i and deletion of N187 at subsequent time points. However, an N-linked glycan site was introduced at 188.3 by the D188.3N mutation.

These data show that the V1V2 evolved through deletions associated with the removal of N-linked glycan sites, in sub-lineage 1, while, in contrast, insertions in this variable region in sub-lineage 2 introduced N-inked glycan sites.

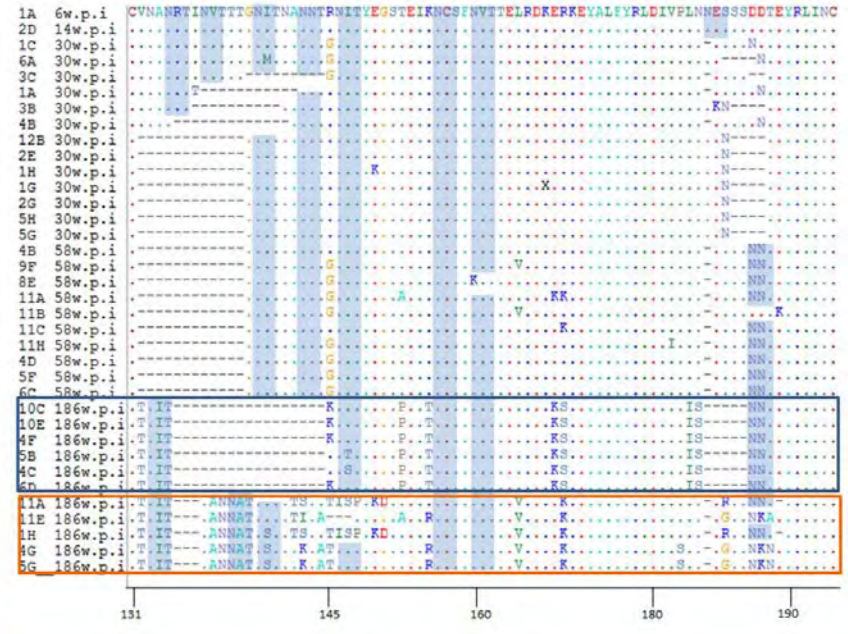

Figure 3.11. Amino acid highlighter analysis of the V1V2 of HIV-1 envelope over time. The blue and orange boxes separate the two sub-lineages circulating at 186 w.p.i. Sub-lineage1 is shown in the blue box, and sub-lineage 2 in the orange. Amino acid identity is shown as dots (.), deletions as dashes (-). The blue bars represent potential N-linked glycan sites. HXB2 numbering is shown below the alignment.

The alpha-2 helix in the C3 region is a target of strain-specific neutralizing antibodies in subtype C HIV-1 infection and variations in this epitope have been shown to confer neutralization escape [145]. The C3 and V4 regions are in close proximity on Env and form a conformational epitope targeted by the strain-specific neutralizing antibodies [146]. In the C3V4 region most of the persistent changes were due to point mutations

(**Figure 3.12**). Of note, the S334N and N336T mutations shifted the PNLG site from 332 to 334 at 186 w.p.i. This region is a common target of bnAbs that target the V3 glycan supersite [147]. The E337K introduced a positive charge. More charge changes were introduced by the mutations E337K, E347K and K348E. Sub-lineage 2 at 186 w.p.i had an R348K mutation that did not modify the charge, but could potentially interfere with binding of nAbs by steric hindrance, owing to the bulkier structure of R when compared to K. The N-linked glycan site at 359 shifted to 357 through the mutations D357N and N359T/S in 4/10 sequences at 58 w.p.i. This glycan was completely removed in sub-lineage 1 at 186 w.p.i, but maintained in sub-lineage 2 at the initial position 359. This provided further evidence that sub-lineage 1 and 2 followed different escape pathways. Between positions 404 and 415, sub-lineage 1 had a six amino acid insertion that results in introduction of an N-linked glycan site. Sub-lineage 2 had a three amino acid insertion that added an N-linked glycan site.

In conclusion, these data show a gradual increase in divergence from the t/f sequence, and an increase in env diversity after detection of neutralizing antibodies. Most of the diversity was attributed to changes in the V1V2 region along with the C3V4 region, and were thus proposed to be putative antibody targets to strain specific nAbs. The difference in the sub-populations at 186 w.p.i in both the V1V2 and C3V4 regions suggested that the viral populations were diversifying under two sources of selective pressure, possibly neutralizing antibodies with different specificities; or viruses were exploring two separate pathways to escape a single specificity. The various potential escape mutations presented here show the complexity of escape pathway employed by the virus.

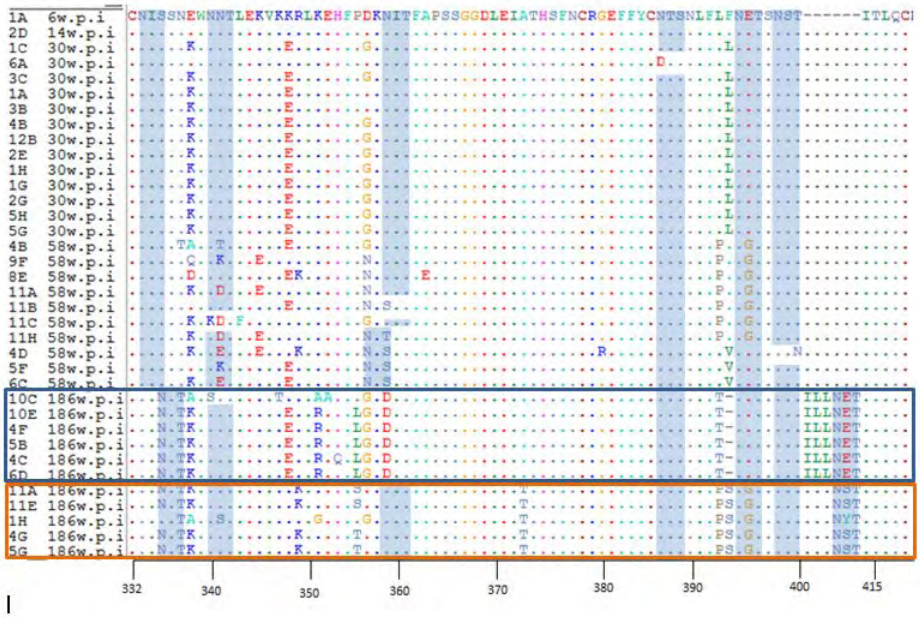

Figure 3.12. Amino acid highlighter analysis of the C3V4 of HIV-1 envelope over time. There were two sub-lineages at 186 w.p.i shown in the blue box (sub-lineage 1) and orange box (sub-lineage 2). The blue vertical bars represent N-linked glycan sites. HXB2 numbering is shown below the alignment. Amino acid identity is shown as dots (.), deletions as dashes (-).

3.6 Neutralization sensitivity of later viruses

To evaluate the different effects of viral evolution on neutralization sensitivity, one representative SGA amplicon was selected from each of the lineages at: 30, 58 and 186 w.p.i, indicated on the phylogenetic tree (**Figure 3.6**). The representative amplicons were chosen based on having the most number of mutations in the population, and therefore representing the most potential escape mutations. Neutralization sensitivity was not evaluated for the 14 w.p.i viruses due to the low

sequence variation and limited evidence of selection between this time point and the t/f sequences. We thus expected that the antibody kinetics would not be significantly different from the t/f virus.

Because strain-specific neutralizing antibodies target the virus that elicited them, we expected that the antibodies produced in response to the t/f virus would be ineffective against the 30 w.p.i viral variant. Likewise, the antibodies targeting the 30 w.p.i variant would likely not neutralize the escaped virus at 58 w.p.i. Furthermore, it is well documented that generally there is little to no contemporaneous neutralization in early infection due to rapid nature of viral escape [148] [149]. We would thus expect that the neutralization curves to shift incrementally to the right to reflect contemporaneous escape. The generated representatives of envelopes from the different time points were tested against plasma spanning the first year of infection (**Figure 3.13**).

No contemporaneous neutralization was observed up until 30 weeks, at which point a very low level of contemporaneous neutralization was detected. As expected, viruses were neutralized by serum collected after virus sampling (**Figure 3.13A**). At the first time point where breadth was detected (58 w.p.i), there was evidence of modest sensitivity to contemporaneous neutralization (ID_{50} 1:94). The t/f virus was the most sensitive clone, all the viral variants that emerged later were less sensitive to neutralization (**Figure 3.13B**). There was an increase in titer to CAP292_30w.p.i such that CAP292_30 w.p.i became more sensitive to neutralization than the t/f virus by 58 w.p.i. As expected, CAP292_186w.p.i was resistant throughout the time span tested.

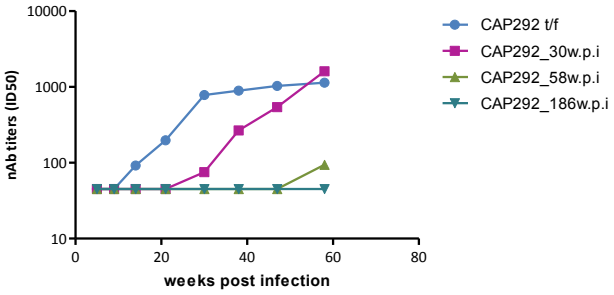

Figure 3.13. Neutralization sensitivity of CAP292 viruses in the first year post infection. This graph shows the kinetics of the responses at various time points within the first year of infection against the t/f, 30 week, 58 week and 158 week clones

These data show sequential escape from neutralizing antibodies, with low level contemporaneous neutralization of the CAP292_58 w.p.i virus illustrating incomplete escape at this time point. A high titer responses had developed by 30 w.p.i, which may be due to maturation of the nAb lineage, or the development of additional nAb responses to the virus.

3.7 Putative strain-specific neutralizing antibody targets

Our sequence data analysis showed changes in the length and glycosylation of the V1V2 over time. Additionally, the C3V4 region evolved by amino acid charge changes and shift in the N-linked glycan sites. Although there were other mutations in the other regions of Env, the V1V2 and the C3V4 regions have been identified as common targets for strain-specific neutralizing antibodies [104]. We thus focused our attention of

these regions, and generated chimeric viruses to investigate whether the V1V2 and C3V4 regions were strain-specific neutralizing antibody targets in CAP292.

The chimeras were generated by introducing the V1V2 and C3V4 from CAP292 transmitted/founder virus into the envelope of CAP239 which showed resistance to neutralization by CAP292 ssnAb. This was done using two chimera generation strategies (see **Figure 2.5** for the strategies). Using the overlap extension PCR strategy, three fragments (referred to as F1, F2 and F3) of envelope were amplified to make the V1V2 (**Figure 3.14A**) and C3V4 (**Figure 3.14B**) chimeras. F1 and F3 were amplified from an unrelated envelope of CAP239, whilst F2 – the region of interest – was amplified from the CAP292 t/f envelope. F1 and F2 were linked (**Figure 3.14C**), and the resultant fragment (F1F2) was linked with F3 to complete the full length envelope chimera (F1F2F3).

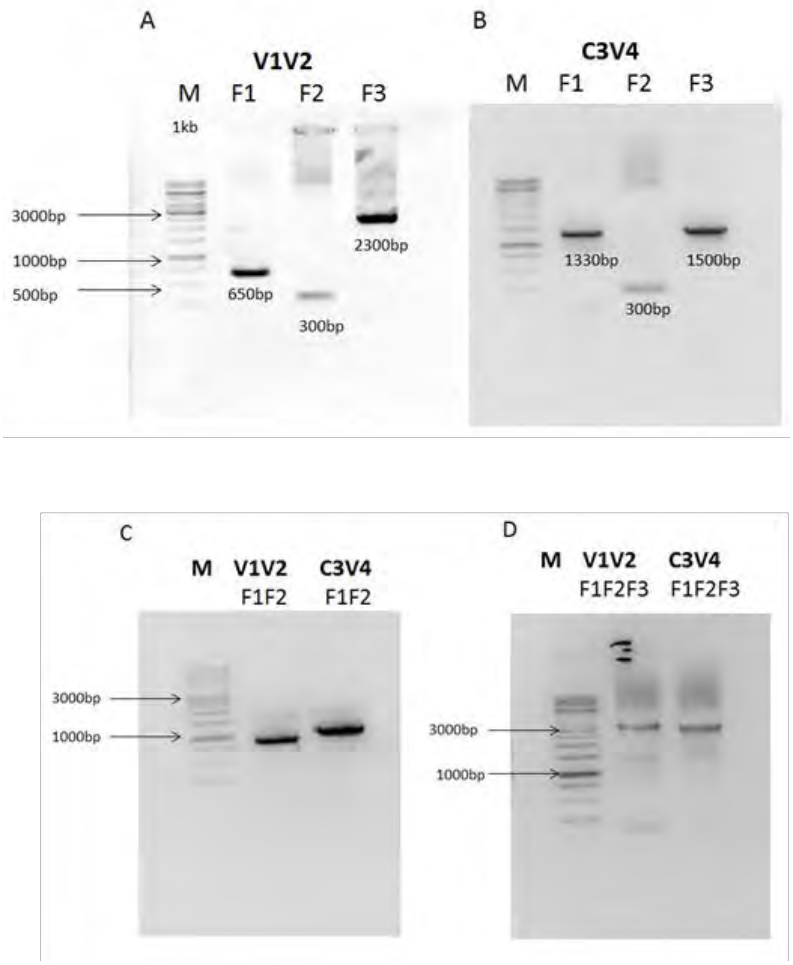

Figure 3.14. Agarose gel (1%) showing amplified fragments generated using the overlap extension PCR. A. Amplified fragments for generation of the V1V2 chimera. B. Amplified fragments for C3V4 chimera generation. C. Linked fragments F1 and F2 to make F1F2. D. F3 linked to F1F2 to complete the chimera (F1F2F3).

An alternative chimera generation strategy – mega primer approach (**Figure 3.15**) – was performed concurrently with the overlapping fragment PCR to improve the chances of successful cloning. In this method, F2 was amplified as above. This

amplicon was then used as a mega primer to make chimeric *env* plasmid. The region of the plasmid corresponding to F2 was replaced with the CAP292 F2 to make the chimeric 8kb envelope plasmid (**Figure 3.15**). This method produced a chimeric *env* plasmid identical to the method above, but required fewer PCR reactions.

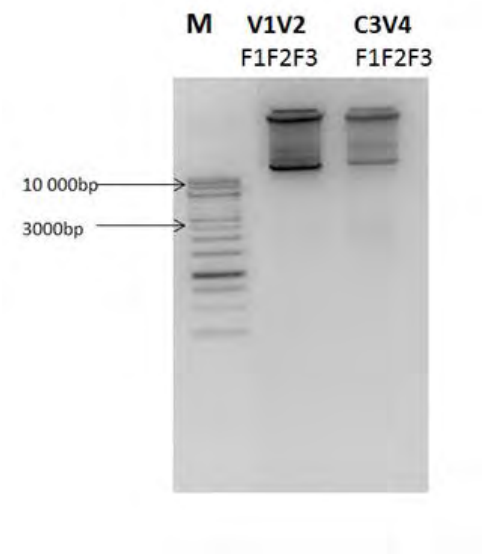

Figure 3.15. 1% Agarose gel showing envelope plasmid amplified using the mega primer approach. The fragments shown are the V1V2 (left) and C3V4 (right) chimeric envelope plasmids.

The DNA bands observed (**Figure 3.15**) were approximately 10kb in size, instead of the expected 8kb. This may have been due to the plasmid being in an open circle conformation, which is known to cause slower migration during gel electrophoresis. Chimeras generated through both strategies were confirmed by Sanger sequencing to have incorporated the correct sequences: F1 and F3 matched the CAP239 *env*, and F2 matched the CAP292 *env*. The sequences of the chimeras generated through the

mega primer approach are shown in **Figure 3.16** and these were used for subsequent experiments.

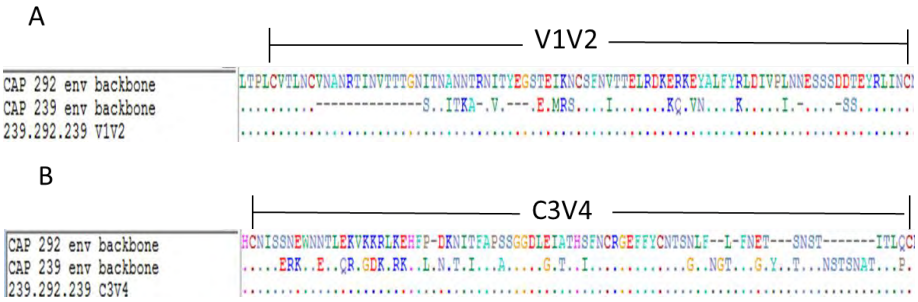

Figure 3.16 Confirmation of chimerism. The sequences of the chimeric viruses 239.292.239_V1V2 in (**A**) and 239.292.239_C3V4 in (**B**) are aligned to the CAP 292 and CAP 239 *env* backbones. In both instances, the sequence of the chimeric virus matches that of the CAP 292 backbone in the specified regions.

Chimeric pseudoviruses were generated from the chimeric *env* plasmids and tested against plasma spanning the first year of infection in neutralization assays. The insertion of CAP292 V1V2 into the neutralization resistant CAP239 backbone to make the 239.292.239_V1V2 chimera, showed acquisition of sensitivity to neutralization after 21 w.p.i, but was less sensitive than the CAP292 t/f virus (**Figure 3.17**). Similarly, the C3V4 region inserted into the CAP239 backbone to make the 239.292.239_C3V4 chimera introduced sensitivity into the CAP239 virus (**Figure 3.17)**

The curve of 239.292.239_C3V4 chimera showed neutralization sensitivity at 14 w.p.i, similar to the curve of the t/f virus, suggesting that the initial antibody response targeted the C3V4 regions. The fact that the response did not recapitulate that of the t/f virus, suggested that there might have been other antibody specificities during this time. The

initial response was followed by a response to the V1V2 regions 7 weeks later. At 21 w.p.i, the sum of the titers (ID_{50} 1:728 and ID_{50} 1:939) amounted to titers comparable to those acquired for the t/f virus (ID_{50} 1:1568), recapitulating the response to the t/f. This suggested that both anti-C3V4 and anti-V1V2 antibodies were responsible for neutralization. The responses peaked at 30 and 38 weeks for C3V4 and V1V2 respectively, with the V1V2 levelling at a lower titer compared to C3V4. These results suggest that both these regions were targeted by the strain specific response during acute infection.

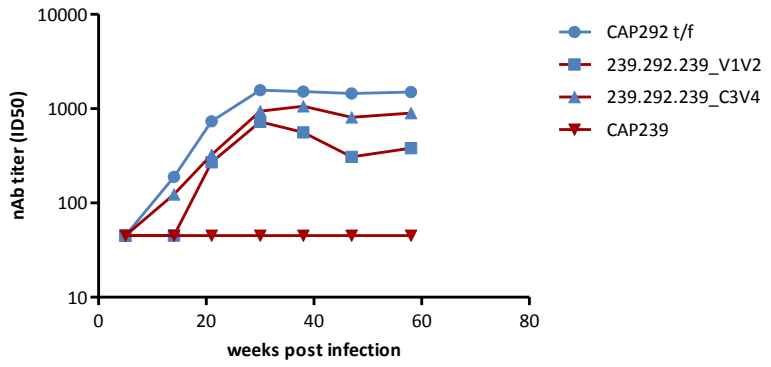

Figure 3.17. Mapping the strain-specific response in CAP292. The generated chimeras were tested against plasma spanning the first year of infection. The nAb titers are represented over time.

As the backbone can influence the presentation of epitopes, chimeras were constructed to determine whether mutation within these regions mediated escape. CAP292_30 w.p.i escaped virus was used as the *env* backbone (**Figure 3.18**). These chimeras were generated by replacing the V1V2 and C3V4 of the CAP 292_30 w.p.i virus with the same region from the neutralization sensitive CAP292 t/f virus. In this

way, we were able to generate a virus with the t/f V1V2 (30w.p.i.t/f_V1V2.30w.p.i) and the 30 w.p.i virus with the t/f C3V4 (30w.p.i.t/f_C3V4.30w.p.i). The representative pseudoviruses were tested against plasma from the first year of infection. The 30w.p.i.t/f_V1V2.30wpi chimera almost entirely overlapped with the t/f neutralization curve suggesting that escape from V1V2 response shown to emerge at 21 weeks post infection is nearly entirely mediated by V1V2 by 30 w.p.i. In contrast, only partial escape from the C3V4 response is mediated by changes in C3V4 of the 30 week clone, suggesting additional escape mutation elsewhere. This also suggested that the mutations acquired by CAP292_30w.p.i mediated escape. The chimeric virus recapitulated the initial response to the infecting virus by 38 w.p.i and become more sensitive by 58 w.p.i, suggesting the V1V2 region was the sole target of antibodies at this time. There was a slight acquisition of sensitivity in the 30w.p.i.t/f_C3V4.30w.p.i chimeric virus at 30 w.p.i, suggesting that C3V4 targeting antibodies had begun to emerge at this time. Additionally, this suggested that the mutations acquired in the C3V4 region mediated partial viral escape.

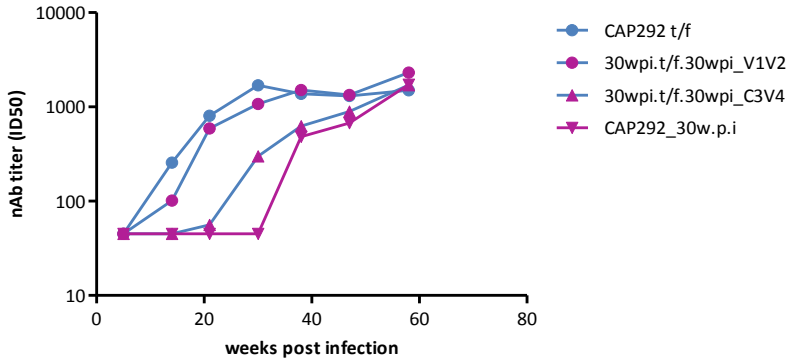

Figure 3.18. Neutralization curves of chimeric viruses using CAP292_30w.p.i as the *env* backbone. nAb titers are presented

These results, using the native CAP292_30w.p.i backbone, differed somewhat from those where the CAP292 backbone was used. Namely, the C3V4 responses appear to be much greater for the CAP239 backbone chimeras, such that the C3V4 is implicated is the initial antibody target. The table below shows the differences in the characteristics between the two backbones used, which may be responsible for the differential neutralization sensitivity.

Table 1. Variable loop characteristics of the two Env backbones used for chimera generation

	CAP292_30w.p.i backbone			CAP239 backbone		
Env region	length	PNLGs	charge	length	PNLGs	charge
V1	24	3	2	18	2	0
V2	39	1	-1	41	2	1
V3	35	1	5	35	1	5
V4	21	3	-1	31	6	0
V5	10	1	0	13	2	3

Because the CAP292 backbone was close to the native virus, the data from the CAP292 backbone chimeras was given greater weight. Thus, these data suggested that the V1V2 region was major target of the strain-specific neutralizing response in CAP292. The partial sensitivity of the C3V4 chimeric virus suggested that low titer neutralizing antibodies targeting the C3V4 region emerged later on during infection.

3.8 Mapping amino acid residues targeted by the broadly neutralizing response in CAP292

The role of viral evolution in the development of bnAb targets has been demonstrated (reviewed by Moore, Williamson & Morris [150]). Viral epitopes targeted by strain specific neutralizing antibodies may evolve to become targets for the broadly neutralizing response through immune escape. We have shown that escape from the strain-specific responses in CAP292 occurred through insertion, deletions and glycan shift in the V1V2 and the C3V4 regions. We thus aimed to map the bnAb response to assess the relationship between the epitopes targeted by strain specific and broadly neutralizing responses.

Longitudinal SGA sequence data was generated to evaluate evolution in amino acid residues known to play a crucial role in neutralization by broadly neutralizing monoclonal antibodies. Sites were identified as putative bnAb targets if the nonsynonymous mutations occurred in a known bnAb site, in more than 50% of the sequences at 186 w.p.i —when the broadly neutralizing response peaked. The following sites were identified as putative bnAb escape sites in CAP292: L165 and E169 in V2; N332 in C3; a site between 463 and 464 in V5, D674 and R683 in MPER.

In V2, an L165V mutation was first introduced at 58 w.p.i and increased in frequency at 186 w.p.i. (**Figure 3.19**). Of the sequences at 186 w.p.i, sub-lineage 1 (blue box) had the wildtype L165 together with the E169K mutation while sub-lineage 2 had the L165V mutation. These sites are known to be targeted by the PG9/16 class of mAbs.

The site identified in the C3 region at position 332, is a well-known target of the PGT128 class of bnAbs (**Figure 3.19**) [113 117 151] . The presence of the N-linked glycan site in the t/f sequence, and the maintenance of this site until 58 w.p.i suggests that

the initial antibody response (ssnAbs) did not target N332 (**Figure 3.19**). However, two escape mutations, S334N and N336T that were introduced at 186 w.p.i resulted in a shift of the N-linked glycan site from 332 to 334, indicating that this site may have been targeted by later bnAbs.

The shift of the N-linked glycan site from 464 to 463.1 in the V5 occurred in the CD4 binding site. The shift may render the sub-lineage 1 resistant to the CD4-binding antibodies **(Figure 3.19**). The last sites identified were in MPER at positions 674 and 683 (**Figure 3.19**). The mutations occurred in a region overlapping the 4E10 and 10E8 anti-MPER monoclonal antibodies epitopes and where found in the viral variants that make up sub-lineage 2 at 186 w.p.i. This suggested MPER-like antibodies to the sub-lineage 2 viral population.

The pattern of mutations observed here suggested viruses escaped through multiple pathways.

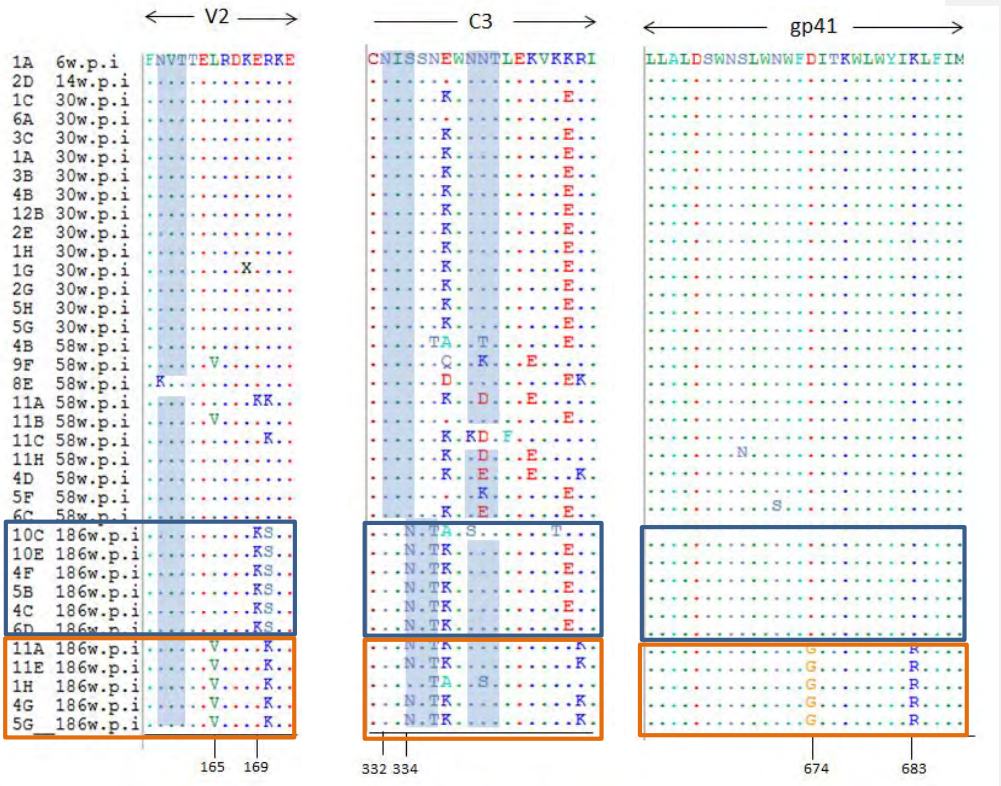
V2
C3
gp41
1A 6w.p.i FNVTTELRDKERKE
2D 14w.p.i
1C 30w.p.i
6A 30w.p.i
3C 30w.p.i
1A 30w.p.i
3B 30w.p.i
4B 30w.p.i
12B 30w.p.i
2E 30w.p.i
1H 30w.p.i
1G 30w.p.i
2G 30w.p.i
5H 30w.p.i
5G 30w.p.i
4B 58w.p.i
9F 58w.p.i
8E 58w.p.i
11A 58w.p.i
11B 58w.p.i
11C 58w.p.i
11H 58w.p.i
4D 58w.p.i
5F 58w.p.i
6C 58w.p.i
10C 186w.p.i
10E 186w.p.i
4F 186w.p.i
5B 186w.p.i
4C 186w.p.i
6D 186w.p.i
11A 186w.p.i
11E 186w.p.i
1H 186w.p.i
4G 186w.p.i
5G 186w.p.i
CNISSNEWNNTLEKVKKRI
LLALDSWNSLWNWFDITKWLWYIKLFIM
165
169
332
334
674
683

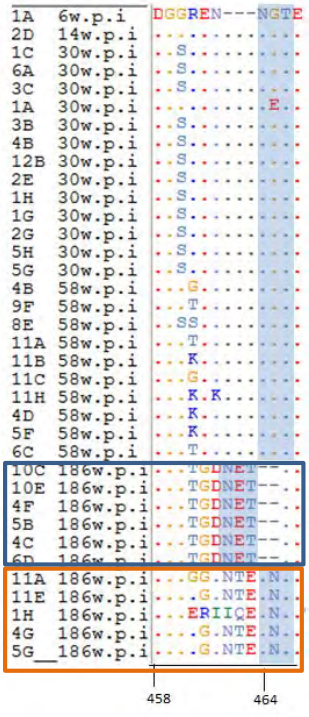

Figure 3.19. Identifying broadly neutralizing antibody targets. Amino acid highlighter showing sequences variation in putative broad neutralizing antibody sites in the V2, C3, V5 and gp41 regions. HXB2 numbering of the sites undergoing evolution are shown below the highlighter plots. Blue bars indicate potential N-linked glycan sites. Sub-lineage 1 sequences are enclosed in the blue box and sub-lineage 2 sequences in the orange box.

To identify whether any of these sites were targeted by the broad response in CAP292, we acquired various mutant viruses from the National Institute of Communicable Disease (L. Morris, National Institute of Communicable Diseases). These included two constructs with alanine substitutions, representing the L165A and N332A mutants in a conC backbone. The D674 construct was mutated to D674S in a Cot6 backbone. The neutralization kinetics of the both the mutant viruses and the wildtype backbone viruses were tested against longitudinal CAP 292 plasma. The fold difference in neutralization titer for the mutant and wildtype was calculated by dividing the ID_{50} of the wildtype virus by that of the mutant virus with a fold difference above one indicating an increase in

neutralization sensitivity, whereas a fold difference below one indicated a decrease in neutralization potential epitopes were identified as a fold increase above one indicating an increase in neutralization sensitivity, whereas the reduction in neutralization sensitivity was identified as viral escape indicated by a fold difference below one.

The introduction of the L165A mutation resulted in increased neutralization sensitivity compared to wild-type conC wildtype virus at all time points over the three year time period (**Figure 3.20)**. A similar observation was made by Wibmer et al.[152] where conC L165A was more sensitive to neutralization than the conC wildtype when tested against plasma of CAP257, of the CAPRISA cohort, suggesting that this mutation may change the conformation of Env, perhaps results in exposure of binding antibody epitopes.

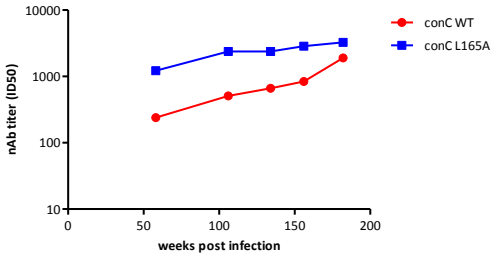

w.p.i	58	106	134	156	182
conC WT	239.59	509.14	662.93	839.93	1896.7
conC L165A	1216.31	2375.8	2372.52	2859.94	3265.58
ID_{50} fold change	0.019	0.21	0.27	0.29	0.58

Figure 3.20. Neutralization plots of the L165A mutant virus vs the conC wildtype. The neutralization titers at each time point are shown in the table. The ID50 fold change was calculated as the neutralization titer of the wildtype virus divided by that of the mutant virus.

The conC wildtype and the N332A mutant viruses had similar neutralization titers until the 186 w.p.i, when the broadly neutralizing antibody response peaked. At this time point, the conC wildtype virus (containing the glycan site at 332) was 2.5 fold more sensitive to neutralization than the N332A mutant virus (**Figure 3.21)**. This suggested that the circulating antibodies required the N332 glycan for neutralization, however only differences greater than 3 fold are considered relevant, given the error of the assay.

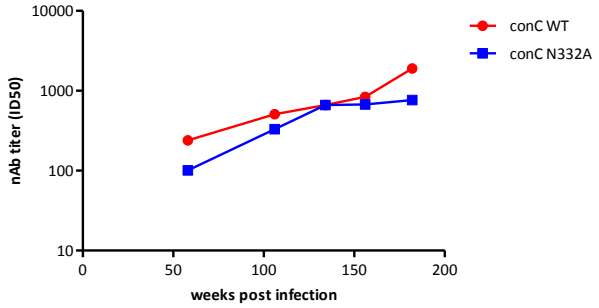

w.p.i	58	106	134	156	182
conC WT	239.59	509.14	662.93	839.93	1896.7
conC N332A	101.06	330.63	662.93	674.09	765.55
ID_{50} fold change	2.4	1.5	1	1.24	2.5

Figure 3.21. Neutralization plots of the N332A mutant virus vs the conC wildtype. The neutralization titers at each time point are shown in the table. The ID_{50} fold change was calculated as the neutralization titer of the wildtype virus divided by that of the mutant virus.

Neutralization sensitivity assessment of the Cot6 D674S and Cot6 wildtype showed no significant effect on neutralization up to 182 w.p.i, with a slight reduction in

neutralization of 2.27- fold and 1.7-fold at 106 w.p.i and 182 w.p.i, respectively (**Figure 3.22**). This suggested the presence of minor neutralizing responses towards D674 developing late in infection.

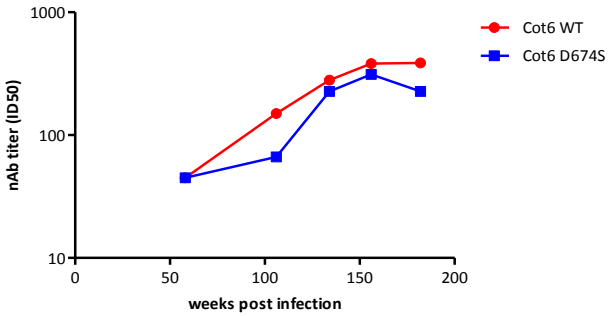

w.p.i	58	106	134	156	182
Cot6 WT	45	150.05	280.52	382.67	386.32
Cot6 D674S	45	66.46	226.72	311.67	227.22
ID_{50} fold change	1	2.27	1.2	1.227	1.7

Figure 3.22. Neutralization plots of the D674S mutant virus vs the cot6 wildtype. The neutralization titers at each time point are shown in the table. The ID_{50} fold change was calculated as the neutralization titer of the wildtype virus divided by that of the mutant virus.

The reduction in neutralization that resulted from the N332A mutation, suggested that at least some of the bnAb response in CAP292 was directed toward the C3 region. Furthermore, there was some evidence of low level neutralization toward the MPER, given the slight reduction in neutralization due to the D674S mutation. Together these

data suggest that the broad neutralizing response in CAP292 may have multiple specificities.

4 Discussion and Conclusion

It is generally accepted that an effective HIV-1 vaccine would need to elicit broadly neutralizing antibodies (bnAbs) to block viral infection, and to overcome the extensive global HIV-1 diversity (reviewed by Stamatatos, Morris, Burton & Mascola [153]). However, the development of such a vaccine has been elusive. One way to get insights into the development of bnAbs is to elucidate how these responses evolve *in vivo*. It is thought that pressure from the strain-specific neutralizing antibody response drives viral evolution towards epitopes that would later be targeted by bnAbs [154 155]. It is therefore of interest to understand whether the early strain-specific antibodies (ssnAbs) evolve into broadly neutralizing antibodies. This study aimed to determine if a relationship existed between the epitopes targeted by ssnAb and bnAb in CAP292. We hypothesized that if ssnAbs evolved into bnAbs, they would target the same epitopes.

Our data showed that the early strain-specific response targeted the V1V2 region in CAP292, with a C3V4 response possibly emerging at about 30 w.p.i. The data also showed that the mutation acquired in the V1V2 region mediated complete escape, whilst those in the C3V4 mediated partial viral escape. Viral escape occurred after detection of the ssnAb response resulting in viruses harvested after this time point being less sensitive to neutralization than the t/f virus. Although we were unable to conclusively determine the targeted epitope of the broad neutralizing response, the bnAb mapping, together with the pattern of putative escape mutations, suggested that the C3 glycan (N332) and the MPER were possible targets. Due to time constrains, and the confounding effect of the 165 mutation, we were not able to effectively interrogate the presence of V1V2 bnAb specificities. Thus, while the V1V2 region was

targeted by ssnAbs, we could not confirm whether this was also the case for the later bnAb antibodies.

The genetic characterisation of the *env* of the t/f virus provided a baseline from which to track evolution, and provided information on the virus that primed the immune response in infected individuals. In CAP292, consistent with infection with a single variant infection, we found that early sequences had a distribution of hamming distances that conformed to the Poisson model, with a star-like phylogeny. There were however slight deviations from the model with some sequences harbouring shared mutations (**Figure 3.4**) suggesting a selective immune pressure at the time of sampling.

Similar to another study by Gray *et al*.[156], CAP292 developed potent neutralizing antibodies (over 1:1000, **Figure 3.5**) within the first year of infection, and these antibodies had no impact on viral replication. Typical of HIV-1 subtype C infection, the specificity of the strain-specific response was mapped to the V1V2 [157] [158]. Mapping of C3V4 generated some discrepancies using different Env backbones with the C3V4 chimera in the CAP239 backbone, showing a greater neutralization sensitivity as compared with the C3V4 chimera in the CAP292 backbone. These differences are likely a result of differential conformations of the envelope between the two backbones [159]. Studies have shown that higher N-linked glycan density and longer variable loops are associated with neutralization resistant viruses [160] [112], and the differences in these features between the two backbones may have impacted the Env conformation, resulting in the C3V4 epitope being more accessible in the CAP239 backbone V1V2 (**Table 1**). Additionally, the mutations found in the backbones may have differing effects on neutralization sensitivy. For more premise mapping of antibody targets, the

mutations would have to be individually tested to identify each of their contribution to neutralization sensitivity.

We detected low level variation before neutralizing antibodies first emerged. This could be attributed to the pressure exerted by either CTL [84], or by non-neutralizing antibodies. Although it is difficult to defintively rule out CTL pressure, these mutations did not occur in known CTL epitopes associated with CAP292's HLA profile (A 29:02. 30:01; B15:03, 44:03, C 2:10, 02:10). However the variation did occur in sites in the V5 and gp41 regions that have been shown to evolve in response to ADCC-mediating antibodies [161] [162] [163]. However, if there was pressure from the ADCC-mediating antibodies, it was temporal as these variations did not persist after the emergence of the nAb response. Further research would need to be conducted to determine the impact of the non-neutralizing antibodies on viral evolution.

Similar to other studies, we identified the V1V2 as a major contributor to Env evolution and this region was shown to be a determinant of sensitivity to neutralization (**Figure 3.10**). In CAP292 the V1V2 variable loop became shorter with time, and this was associated with a reduction in the number of N-linked glycan sites. Interestingly, viruses with the shorter V1V2 variable loops and less number of glycan sites were generally more resistant to neutralization, which is in contrast to the observation made by others [160] [112].

Interestingly, we identified two sub-lineages, at the peak of the broadly neutralizing response, with distinct sequence differences across V1V2, C3V4 and MPER (**Figure 3.11 & 3.12**). This pattern of viral evolution has been demonstrated [148], however whether this occurs as a result of two routes of escape from the same antibody specificity, or multiple antibodies with different specificities has not been investigated.

These data highlights the complexity of viral evolution leading to the development of the broadly neutralizing antibodies response. Identifying the neutralization sensitivity of each of these subpopulations in CAP292 would provide valuable insight into the dynamics of viral evolution in CAP292, while determining the impact of this on the bnAb response would be of particular interest.

There are a number of amino acids that have been shown to be critical for bnAbs recogntion. Three sites (N160, L165 and K169) have been identified as crucial for neutralization by PG9/16 broad neutralizing monoclonal antibodies (mAbs) [164]. In CAP292, we identified mutations at L165V and E169K at the peak of the broadly neutralizing response. The L165V mutation occurred in sub-lineage 2 whilst the E169K mutation occurred in sub-lineage 1. Contrary to our expectations, the L165A mutant virus was more sensitive to neutralization than the wildtype (**Figure 3.19**) possible due to the more compact structure of alanine (A), compared to lysine (K), resulting in an epitope being more exposed allowing easier access by the neutralizing antibodies, or that this change somehow affected the larger conformation of the loop, resulting exposing a non-neutralizing epitope. Time constrains did not allow the interrogation of the E169K mutation in sub-lineage 1, which may help clarify whether a PG9/16 specificity is present in CAP292. However, the K (lysine) is known as the desired amino acid residue for PG9/16-like antibodies [165]. The reversion from E to K may suggest the presence of antibodies targeting the K169 in the donor drove , and that this kind of antibody pressure was not present in CAP292.

CAP292 may also have developed PGT128-like antibodies. These antibodies typically recognise a glycan patch which includes sites N301, N332 and N325 [147]. The most important target of these antibodies is the glycan at position 332. The shift of the glycan from N332 to N334 in CAP292 suggested the presence of PGT128-like

antibodies. Our bnAb mapping data suggested that the N332A mutation resulted in an increase in neutralization resistance, further supporting PGT128-like specificities in CAP292. The sites D674 and N671 have been shown to be crucial for neutralization by an anti-MPER mAb Z13e1 [166]. However, neutralization sensitivity was not greatly impacted using the D674S mutant virus. While these mutations occurred in sites confirmed as important for certain mAbs, this study was preliminary more site-directed mutant viruses would need to be tested to map the specificity of the broadly neutralizing response to single amino acids.

Conclusion

This study tracked viral evolution over three key time points during antibody maturation: firstly at 14 w.p.i when the first strain-specific response emerged, followed by a possible second wave of antibodies to the 30_w.p.i virus, and eventually the development of the broad response at 58 w.p.i. A single virus established clinical infection in CAP292 and there was limited evolution observed before the development of strain-specific neutralizing antibodies, which targeted the V1V2 region. Antibody pressure to the V1V2 was maintained throughout the period of infection studied, and resulted in genetically diverse viral variants.

Two viral escape pathways were established by the peak of the bnAb response. Our data shows that the broad response targeted the C3 N332 glycan. The MPER and the V1V2 region may have been targeted by bnAb responses, however, further work is required to confirm this. If this work confirms a V1V2 bnAb target, this would provide good support for a relationship between early ssAb responses and later bnAb specificities.

The pathway that leads to the development of broadly neutralizing antibodies is dynamic and influenced by the interactions between viral and host immune factors. This study showed the plasticity of Env in response to the neutralizing antibody pressure, and that a relationship between strain specific and broad neutralizing epitopes may exist. Molecular characterization of the antibody response is needed to determine the full extent of the antibody-virus interaction to gain insights into development of breadth in this individual.

5 Appendices

5.1 Appendix A: Primer sequences

Primer Name	Sequence (5'-3')
Vif1	GGGTTTATTACAGGGACAGCAGAG
OFM19	GCACTCAAGGCAAGCTTTATTGAGGCTTA
EnvArx	CACCGGCTTAGGCATCTCCTATAGCAGGAAGAA
EnvN	TTGCCAATCAAGGAAGTAGCCTTGTGT
EnvM	TAGCCCTTCCAGTCCCCCCTTTTCTTTTA
EnvA	GGCTTAGGCATCTCCTATAGCAGGAAGAA
V1V2.F1.rev	GAGTGGGGTCAACTTTACACATGGCTTGAG
V1V2.F2.for	GTTGACCCCACTCTGTGTCACTTTAAATTGT
V1V2.F2.rev	GGACAGGCTTGTTTTATGGCTGAGGTATTAC
V1V2.F3.for	CAAGCCTGTCCAAAGGTAACTTTTGATCC
C3V4.F1.rev	CACTCATTACTACTGATGTTACAATGTGCTTGTC
C3V4.F2.for	TGTAACATCAGTAGTAATGAGTGGAACAATAC
C3V4.F2.rev	GGCATACATTGCTTGTCCTACCTTCTG
C3V4.F3.for	CAATGTATGCCCCTCCCATTGCAGGAAAC
EF00	GGGAAAGAGCAGAAGACAGTGGCAATGA
EF15	CTTGCTCTCCACCTTCTTCTTC
EF55	GCCCCAGACCGTGAGTTGCAACATATG
EF115	AGAAAAATTCCCCTCCACAATTAA
EF170	AGCAGGAAGCACTATGGG
EF175	TTTAGCATCTGATGCACAGAATAG

EF200	GGGATAACATGACCTGGATGCAGTGGG
EF260	TTCAGCTACCACCGATTGAGAGACT
FOR14	TATGGGACCAAAGCCTAAAGCCATGTG
FOR16	TTTAATTGTGGAGGAGAATTTTTCTA
REV15	CTGCCATTTAACAGCAGTTGAGTTGA
REV19	ACTTTTTGACCACTTGCCACCCAT

6 References

1. Joint United Nations Programme on HIV/AIDS (UNAIDS). AIDS by the numbers. *Jc2571/1/E* 1–11 (2015). doi:JC2571/1/E

2. Tebit, D. M. & Arts, E. J. Tracking a century of global expansion and evolution of HIV to drive understanding and to combat disease. *Lancet. Infect. Dis.* **11,** 45–56 (2011).

3. Connor, E. M. *et al.* The New England Journal of Medicine Downloaded from nejm.org at UNIV OF CAPEWN LIBRARIES on November 24, 2014. For personal use only. No other uses without permission. Copyright © 1994 Massachusetts Medical Society. All rights reserved. *N. Engl. J. Med.* **331,** 1173–1180 (1994).

4. Guay, L. A. *et al.* Intrapartum and neonatal single-dose nevirapine compared with zidovudine for prevention of mother-to-child transmission of HIV-1 in K ampala , Uganda : HIVNET 012 randomised trial. *Lancet* **354,** 795–802 (1999).

5. Grant, R. M. *et al.* Preexposure chemoprophylaxis for HIV prevention in men who have sex with men. *N. Engl. J. Med.* **363,** 2587–2599 (2010).

6. Cohen, M. S. *et al.* Prevention of HIV-1 infection with early antiretroviral therapy. *N. Engl. J. Med.* **365,** 493–505 (2011).

7. Thigpen, M. C. *et al.* Antiretroviral Preexposure Prophylaxis for Heterosexual HIV Transmission in Botswana. *N. Engl. J. Med.* **367,** 423–434 (2012).

8. Donnell, D. *et al.* Heterosexual HIV-1 transmission after initiation of antiretroviral therapy: a prospective cohort analysis. *Lancet* **375,** 2092–8 (2010).

9. The Hiv-causal Collaboration. The effect of combined antiretroviral therapy on the overall mortality of HIV-infected individuals. *AIDS* **24,** 123–137 (2010).

10. Cohen, M. S. *et al.* NEW ENGLAND JOURNAL. *N. Engl. J. Med.* **365,** 493–505 (2011).

11. Baeten, J. M. *et al.* Antiretroviral Prophylaxis for HIV Prevention in Heterosexual Men and Women. *N. Engl. J. Med.* **367,** 399–410 (2012).

12. Reynolds, S. J. *et al.* NIH Public Access. *AIDS* **25,** 473–477 (2012).

13. Abdool Karim, Q. *et al.* Effectiveness and safety of tenofovir gel, an antiretroviral microbicide, for the prevention of HIV infection in women. *Science* **329,** 1168–74 (2010).

14. McCormack, S. *et al.* PRO2000 vaginal gel for prevention of HIV-1 infection (Microbicides Development Programme 301): a phase 3, randomised, double-blind, parallel-group trial. *Lancet* **376,** 1329–1337 (2010).

15. Marrazzo, J. M. *et al.* Tenofovir-Based Preexposure Prophylaxis for HIV Infection among African Women. *N. Engl. J. Med.* **372,** 509–518 (2015).

16. Das, M. *et al.* Decreases in community viral load are accompanied by reductions in new HIV infections in San Francisco. *PLoS One* **5,** e11068 (2010).

17. Montaner, J. S. G. *et al.* Association of highly active antiretroviral therapy coverage, population viral load, and yearly new HIV diagnoses in British Columbia, Canada: a population-based study. *Lancet* **376,** 532–9 (2010).

18. Tanser, F., Bärnighausen, T., Grapsa, E., Zaidi, J. & Newell, M.-L. High coverage of ART associated with decline in risk of HIV acquisition in rural KwaZulu-Natal, South Africa. *Science* **339,** 966–71 (2013).

19. (UNAIDS), J. U. N. P. on H. The Gap Report. *Geneva: UNAIDS* (2014). doi:ISBN 978-92-9253-062-4

20. Collins, D. L. & Leibbrandt, M. The financial impact of HIV/AIDS on poor households in South Africa. *AIDS* **21 Suppl 7,** S75–S81 (2007).

21. Beaulière, A. *et al.* The financial burden of morbidity in HIV-infected adults on antiretroviral therapy in Côte d'Ivoire. *PLoS One* **5,** 1–7 (2010).

22. Nozaki, I., Dube, C., Kakimoto, K., Yamada, N. & Simpungwe, J. B. Social factors affecting ART adherence in rural settings in Zambia. *AIDS Care* **23,** 831–8 (2011).

23. Sweeney, S. & Vanable, P. A. The Association of HIV-Related Stigma to HIV Medication Adherence : A Systematic Review and Synthesis of the Literature . *AIDS Behav.* **20,** 29–50 (2016).

24. Kuhns, L. M. *et al.* An Index of Multiple Psychosocial, Syndemic Conditions Is Associated with Antiretroviral Medication Adherence Among HIV-Positive Youth. *AIDS Patient Care STDS* **30,** 683–693 (2016).

25. Peltzer, K., Sikwane, E. & Majaja, M. Factors associated with short-course antiretroviral prophylaxis (dual therapy) adherence for PMTCT in Nkangala district, South Africa. *Acta Paediatr. Int. J. Paediatr.* **100,** 1253–1257 (2011).

26. Pinoges, L. *et al.* Risk Factors and Mortality Associated With Resistance to First-Line Antiretroviral Therapy: Multicentric Cross-sectional and Longitudinal Analyses. *J Acquir Immune Defic Syndr* **68,** 527–535 (2015).

27. Plotkin, S. a. Correlates of protection induced by vaccination. *Clin. Vaccine Immunol.* **17,** 1055–65 (2010).

28. Flynn, N. M. *et al.* Placebo-controlled phase 3 trial of a recombinant glycoprotein 120 vaccine to prevent HIV-1 infection. *J. Infect. Dis.* **191,** 654–65 (2005).

29. Gilbert, P. B. *et al.* Correlation between immunologic responses to a recombinant glycoprotein 120 vaccine and incidence of HIV-1 infection in a phase 3 HIV-1 preventive vaccine trial. *J. Infect. Dis.* **191,** 666–77 (2005).

30. Buchbinder, S. P. *et al.* Efficacy assessment of a cell-mediated immunity HIV-1 vaccine (the STEP STUDY): a double-blinded, randomised, placebo-controlled,

test-of-concept trial. *Lancet* **372,** 1881–1893 (2009).

31. Gray, G. E. *et al.* Safety and efficacy of the HVTN 503/Phambili study of a clade-B-based HIV-1 vaccine in South Africa: a double-blind, randomised, placebo-controlled test-of-concept phase 2b study. *Lancet. Infect. Dis.* **11,** 507–15 (2011).

32. McElrath, M. J. *et al.* HIV-1 vaccine-induced immunity in the test-of-concept Step Study: a case-cohort analysis. *Lancet* **372,** 1894–905 (2008).

33. Rerks-Ngarm, S. *et al.* Vaccination with ALVAC and AIDSVAX to Prevent HIV-1 Infection in Thailand. *N. Engl. J. Med.* **361,** 2209–2220 (2009).

34. Haynes, B. *et al.* Immune-correlates analysis of an HIV-1 vaccine efficacy trial. *Engl. J. Med.* **366,** 1275–1286 (2012).

35. Hammer, S. M. *et al.* Efficacy trial of a DNA/rAd5 HIV-1 preventive vaccine. *N. Engl. J. Med.* **369,** 2083–92 (2013).

36. Esparza, J. A brief history of the global effort to develop a preventive HIV vaccine. *Vaccine* **31,** 3502–18 (2013).

37. Hessell, A. J. *et al.* Broadly neutralizing human anti-HIV antibody 2G12 is effective in protection against mucosal SHIV challenge even at low serum neutralizing titers. *PLoS Pathog.* **5,** e1000433 (2009).

38. Mascola, J. R. The cat and mouse of HIV-1 antibody escape. *PLoS Pathog.* **5,** e1000592 (2009).

39. Hessell, A. J. *et al.* Effective, low-titer antibody protection against low-dose repeated mucosal SHIV challenge in macaques. *Nat. Med.* **15,** 951–4 (2009).

40. Watkins, J. D. *et al.* An anti-HIV-1 V3 loop antibody fully protects cross-clade and elicits T-cell immunity in macaques mucosally challenged with an R5 clade C SHIV. *PLoS One* **6,** e18207 (2011).

41. Barouch, D. H. *et al.* Therapeutic efficacy of potent neutralizing HIV-1-specific monoclonal antibodies in SHIV-infected rhesus monkeys. *Nature* **503,** 224–8 (2013).

42. Pancera, M. *et al.* Structure of HIV-1 gp120 with gp41-interactive region reveals layered envelope architecture and basis of conformational mobility. *Proc. Natl. Acad. Sci. U. S. A.* **107,** 1166–71 (2010).

43. Zhu, P. *et al.* Electron tomography analysis of envelope glycoprotein trimers on HIV and simian immunodeficiency virus virions. *Proc. Natl. Acad. Sci. U. S. A.* **100,** 15812–7 (2003).

44. Willey, R. & Rutledge, R. Identification of conserved and divergent domains within the envelope gene of the acquired immunodeficiency syndrome retrovirus. *Proc. …* **83,** 5038–5042 (1986).

45. Kwong, P. D., Wyatt, R., Sattentau, Q. J., Sodroski, J. & Hendrickson, W. A. Oligomeric Modeling and Electrostatic Analysis of the gp120 Envelope

Glycoprotein of Human Immunodeficiency Virus Oligomeric Modeling and Electrostatic Analysis of the gp120 Envelope Glycoprotein of Human Immunodeficiency Virus. *J. Virol.* **74,** 1961–1972 (2000).

46. Chen, B., Vogan, E., Gong, H. & Skehel, J. Structure of an unliganded simian immunodeficiency virus gp120 core. *Nature* **433,** (2005).

47. Liu, J., Bartesaghi, A., Borgnia, M. J., Sapiro, G. & Subramaniam, S. Molecular architecture of native HIV-1 gp120 trimers. *Nature* **455,** 109–13 (2008).

48. Pancera, M. *et al.* Structure and immune recognition of trimeric pre-fusion HIV-1 Env. *Nature* **000,** (2014).

49. Kwong, P., Wyatt, R., Robinson, J. & Sweet, R. Structure of an HIV gp120 envelope glycoprotein in complex with the CD4 receptor and a neutralizing human antibody. *Nature* **393,** (1998).

50. Nehete, P. N. *et al.* A post-CD4-binding step involving interaction of the V3 region of viral gp120 with host cell surface glycosphingolipids is common to entry and infection by diverse HIV-1 strains. *Antiviral Res.* **56,** 233–51 (2002).

51. Rizzuto, C. & Sodroski, J. Fine definition of a conserved CCR5-binding region on the human immunodeficiency virus type 1 glycoprotein 120. *AIDS Res. Hum. Retroviruses* **16,** 741–9 (2000).

52. Gallo, S. The HIV Env-mediated fusion reaction. *Biochim. Biophys. Acta - Biomembr.* **1614,** 36–50 (2003).

53. Weiss, C. D. HIV-1 gp41: mediator of fusion and target for inhibition. *AIDS Rev.* **5,** 214–21 (2003).

54. Haqqani, A. a & Tilton, J. C. Entry inhibitors and their use in the treatment of HIV-1 infection. *Antiviral Res.* **98,** 158–170 (2013).

55. Kinlock, B. L., Wang, Y., Turner, T. M., Wang, C. & Liu, B. Transcytosis of HIV-1 through vaginal epithelial cells is dependent on trafficking to the endocytic recycling pathway. *PLoS One* **9,** e96760 (2014).

56. Kolodkin-Gal, D. *et al.* Efficiency of cell-free and cell-associated virus in mucosal transmission of human immunodeficiency virus type 1 and simian immunodeficiency virus. *J. Virol.* **87,** 13589–97 (2013).

57. Boeras, D. I. *et al.* Role of donor genital tract HIV-1 diversity in the transmission bottleneck. *Proc. Natl. Acad. Sci.* **108,** E1156–E1163 (2011).

58. Russell, E. S. *et al.* The genetic bottleneck in vertical transmission of subtype C HIV-1 is not driven by selection of especially neutralization-resistant virus from the maternal viral population. *J. Virol.* **85,** 8253–8262 (2011).

59. Carlson, J. M. *et al.* HIV transmission. Selection bias at the heterosexual HIV-1 transmission bottleneck. *Science* **345,** 1254031 (2014).

60. Keele, B. F. *et al.* Identification and characterization of transmitted and early founder virus envelopes in primary HIV-1 infection. **105,** (2008).

61. Salazar-Gonzalez, J. F. *et al.* Deciphering human immunodeficiency virus type 1 transmission and early envelope diversification by single-genome amplification and sequencing. *J. Virol.* **82,** 3952–70 (2008).

62. Abrahams, M.-R. *et al.* Quantitating the multiplicity of infection with human immunodeficiency virus type 1 subtype C reveals a non-poisson distribution of transmitted variants. *J. Virol.* **83,** 3556–67 (2009).

63. Chohan, B. *et al.* Selection for human immunodeficiency virus type 1 envelope glycosylation variants with shorter V1-V2 loop sequences occurs during transmission of certain genetic subtypes and may impact viral RNA levels. *J. Virol.* **79,** 6528–6531 (2005).

64. Sagar, M. *et al.* Selection of HIV variants with signature genotypic characteristics during heterosexual transmission. *J. Infect. Dis.* **199,** 580–589 (2009).

65. Parker, Z. F. *et al.* Transmitted/founder and chronic HIV-1 envelope proteins are distinguished by differential utilization of CCR5. *J. Virol.* **87,** 2401–11 (2013).

66. Bunnik, E. M. *et al.* Adaptation of HIV-1 envelope gp120 to humoral immunity at a population level. *Nat. Med.* **16,** 995–997 (2010).

67. Salazar-Gonzalez, J. Genetic identity, biological phenotype, and evolutionary pathways of transmitted/founder viruses in acute and early HIV-1 infection. *J. …* **206,** 1273–89 (2009).

68. Ping, L.-H. *et al.* Comparison of viral Env proteins from acute and chronic infections with subtype C human immunodeficiency virus type 1 identifies differences in glycosylation and CCR5 utilization and suggests a new strategy for immunogen design. *J Virol* **87,** 7218–33 (2013).

69. Sodora, D. L., Gettie, A., Miller, C. J. & Marx, P. A. Vaginal transmission of SIV: assessing infectivity and hormonal influences in macaques inoculated with cell-free and cell-associated viral stocks. *AIDS Res. Hum. Retroviruses* **14 Suppl 1,** S119–23 (1998).

70. Brenchley, J. M. *et al.* CD4+ T cell depletion during all stages of HIV disease occurs predominantly in the gastrointestinal tract. *J. Exp. Med.* **200,** 749–59 (2004).

71. Team:SUSTC-Shenzhen/Modeling - 2014.igem.org. Available at: http://2014.igem.org/Team:SUSTC-Shenzhen/Modeling. (Accessed: 6th January 2016)

72. Appay, V. & Sauce, D. Immune activation and inflammation in HIV-1 infection : *J. Pathol.* **214,** 231–241 (2008).

73. Li, Q. *et al.* Microarray analysis of lymphatic tissue reveals stage-specific, gene expression signatures in HIV-1 infection. *J. Immunol.* **183,** 1975–82 (2009).

74. Stacey AR *et al.* Induction of a striking systemic cytokine cascade prior to peak viremia in acute human immunodeficiency virus type 1 infection, in contrast to

more modest and delayed responses in acute hepatitis B and C virus infections. *J Virol* **83,** 3719–3733 (2009).

75. Lane, H. C. *et al.* Interferon-alpha in patients with asymptomatic human immunodeficiency virus (HIV) infection. A randomized, placebo-controlled trial. *Ann. Intern. Med.* **112,** 805–11 (1990).

76. Lapenta, C. *et al.* Type I Interferon Is a Powerful Inhibitor of in Vivo HIV-1 Infection and Preserves Human CD4 ♀ T Cells from Virus-Induced Depletion in SCID Mice Transplanted with Human Cells. *Virology* **263,** 78–88 (1999).

77. Asmuth, D. M. *et al.* Safety, Tolerability, and Mechanisms of Antiretroviral Activity of Pegylated Interferon Alfa-2a in HIV-1–Monoinfected Participants: A Phase II Clinical Trial. *J. Infect. Dis.* **201,** 1686–1696 (2010).

78. Sandler, N. G. *et al.* Type I interferon responses in rhesus macaques prevent SIV infection and slow disease progression. *Nature* **511,** 601–605 (2014).

79. Schoggins, J. W. Interferon-stimulated genes: Roles in viral pathogenesis. *Curr. Opin. Virol.* **6,** 40–46 (2014).

80. McNab, F. W., Rajsbaum, R., Stoye, J. P. & O'Garra, A. Tripartite-motif proteins and innate immune regulation. *Curr. Opin. Immunol.* **23,** 46–56 (2011).

81. St Gelais, C., Coleman, C. M., Wang, J.-H. & Wu, L. HIV-1 Nef enhances dendritic cell-mediated viral transmission to CD4+ T cells and promotes T-cell activation. *PLoS One* **7,** e34521 (2012).

82. Naranbhai, V. *et al.* Innate immune activation enhances hiv acquisition in women, diminishing the effectiveness of tenofovir microbicide gel. *J. Infect. Dis.* **206,** 993–1001 (2012).

83. Masson, L. *et al.* Genital Inflammation and the Risk of HIV Acquisition in Women. *Clin. Infect. Dis.* **61,** 260–269 (2015).

84. Goonetilleke, N. *et al.* The first T cell response to transmitted/founder virus contributes to the control of acute viremia in HIV-1 infection. *J. Exp. Med.* **206,** 1253–72 (2009).

85. Wang, Y. E. *et al.* Protective HLA class I alleles that restrict acute-phase CD8+ T-cell responses are associated with viral escape mutations located in highly conserved regions of human immunodeficiency virus type 1. *J. Virol.* **83,** 1845–1855 (2009).

86. Goulder, P. J. R. *et al.* Evolution and transmission of stable CTL escape mutations in HIV infection. **412,** 334–338 (2001).

87. Barouch, D. H. *et al.* Eventual AIDS vaccine failure in a rhesus monkey by viral escape from cytotoxic T lymphocytes. *Nature* **415,** 335–339 (2002).

88. Prince, J. *et al.* Impact of transmitted CTL escape mutations on replicative capacity and HIV pathogenesis in early infection. *Retrovirology* **9,** O57 (2012).

89. Rolland, M. *et al.* HIV-1 Conserved-Element Vaccines: Relationship between

Sequence Conservation and Replicative Capacity. *J. Virol.* **87,** 5461–5467 (2013).

90. Mudd, P. a *et al.* Vaccine-induced CD8+ T cells control AIDS virus replication. *Nature* **491,** 129–33 (2012).

91. Reynolds, M. R. *et al.* Macaques vaccinated with live-attenuated SIV control replication of heterologous virus. *J. Exp. Med.* **205,** 2537–50 (2008).

92. Hansen, S. G. *et al.* Broadly targeted CD8+ T cell responses restricted by major histocompatibility complex E. *Science (80-.).* (2016). doi:10.1126/science.aac9475

93. Fiebig, E. W. *et al.* Dynamics of HIV viremia and antibody seroconversion in plasma donors : implications for diagnosis and staging of primary HIV infection. *AIDS* **17,** 1871–1879 (2003).

94. Tomaras, G. D. *et al.* Initial B-cell responses to transmitted human immunodeficiency virus type 1: virion-binding immunoglobulin M (IgM) and IgG antibodies followed by plasma anti-gp41 antibodies with ineffective control of initial viremia. *J. Virol.* **82,** 12449–12463 (2008).

95. Burton, D. R. *et al.* Limited or no protection by weakly or nonneutralizing antibodies against vaginal SHIV challenge of macaques compared with a strongly neutralizing antibody. *Proc. Natl. Acad. Sci. U. S. A.* **108,** 11181–6 (2011).

96. Lambotte, O. *et al.* Heterogeneous neutralizing antibody and antibody-dependent cell cytotoxicity responses in HIV-1 elite controllers. *AIDS* **23,** 897–906 (2009).

97. Karasavvas, N. *et al.* The Thai Phase III HIV Type 1 Vaccine trial (RV144) regimen induces antibodies that target conserved regions within the V2 loop of gp120. *AIDS Res. Hum. Retroviruses* **28,** 1444–57 (2012).

98. Bonsignori, M. *et al.* Antibody-dependent cellular cytotoxicity-mediating antibodies from an HIV-1 vaccine efficacy trial target multiple epitopes and preferentially use the VH1 gene family. *J. Virol.* **86,** 11521–32 (2012).

99. Rolland, M. *et al.* Increased HIV-1 vaccine efficacy against viruses with genetic signatures in Env V2. *Nature* **490,** 417–420 (2012).

100. Liao, H. X. *et al.* Vaccine Induction of Antibodies against a Structurally Heterogeneous Site of Immune Pressure within HIV-1 Envelope Protein Variable Regions 1 and 2. *Immunity* **38,** 176–186 (2013).

101. Excler, J.-L., Ake, J., Robb, M. L., Kim, J. H. & Plotkin, S. A. Nonneutralizing functional antibodies: a new 'old' paradigm for HIV vaccines. *Clin. Vaccine Immunol.* **21,** 1023–36 (2014).

102. Gray, E. S. *et al.* Neutralizing antibody responses in acute human immunodeficiency virus type 1 subtype C infection. *J. Virol.* **81,** 6187–96 (2007).

103. Li, B. *et al.* Evidence for potent autologous neutralizing antibody titers and compact envelopes in early infection with subtype C human immunodeficiency virus type 1. *J. Virol.* **80,** 5211–8 (2006).

104. Moore, P. L. *et al.* The c3-v4 region is a major target of autologous neutralizing antibodies in human immunodeficiency virus type 1 subtype C infection. *J. …* **82,** 1860–9 (2008).

105. Lynch, R. M. *et al.* The B cell response is redundant and highly focused on V1V2 during early subtype C infection in a Zambian seroconverter. *J. Virol.* **85,** 905–15 (2011).

106. Sagar, M., Wu, X., Lee, S. & Overbaugh, J. Human immunodeficiency virus type 1 V1-V2 envelope loop sequences expand and add glycosylation sites over the course of infection, and these modifications affect antibody neutralization sensitivity. *Society* **80,** 9586–98 (2006).

107. Euler, Z. & Schuitemaker, H. Cross-reactive broadly neutralizing antibodies: timing is everything. *Front. Immunol.* **3,** 215 (2012).

108. Moore, P. L. *et al.* Limited neutralizing antibody specificities drive neutralization escape in early HIV-1 subtype C infection. *PLoS Pathog.* **5,** e1000598 (2009).

109. Su, B. *et al.* Neutralizing antibodies inhibit HIV-1 transfer from primary dendritic cells to autologous CD4 T lymphocytes. *Blood* **120,** 3708–17 (2012).

110. Bar, K. J. *et al.* Early low-titer neutralizing antibodies impede HIV-1 replication and select for virus escape. *PLoS Pathog.* **8,** e1002721 (2012).

111. Lederle, A. *et al.* Neutralizing antibodies inhibit HIV-1 infection of plasmacytoid dendritic cells by an FcγRIIa independent mechanism and do not diminish cytokines production. *Sci. Rep.* **4,** 5845 (2014).

112. Hraber, P. *et al.* Impact of Clade, Geography and Age of the Epidemic on Hiv-1 Neutralization By Antibodies. *J. Virol.* **88,** 12623–12643 (2014).

113. Gray, E. S. *et al.* The neutralization breadth of HIV-1 develops incrementally over four years and is associated with CD4+ T cell decline and high viral load during acute infection. *J. Virol.* **85,** 4828–40 (2011).

114. Doria-Rose, N. a *et al.* Frequency and phenotype of human immunodeficiency virus envelope-specific B cells from patients with broadly cross-neutralizing antibodies. *J. Virol.* **83,** 188–99 (2009).

115. Walker, L. M. *et al.* Broad and potent neutralizing antibodies from an African donor reveal a new HIV-1 vaccine target. *Science* **326,** 285–9 (2009).

116. Yuste, E. *et al.* Simian Immunodeficiency Virus Engrafted with Human Immunodeficiency Virus Type Neutralization , and Survey of HIV-1-Positive Plasma Simian Immunodeficiency Virus Engrafted with Human Immunodeficiency Virus Type 1 (HIV-1) -Specific Epitopes : Replication. *J. Virol.* **80,** 3030–3041 (2006).

117. Walker, L. M. *et al.* A limited number of antibody specificities mediate broad

and potent serum neutralization in selected HIV-1 infected individuals. *PLoS Pathog.* **6,** e1001028 (2010).

118. Dhillon, A. K. *et al.* Dissecting the neutralizing antibody specificities of broadly neutralizing sera from human immunodeficiency virus type 1-infected donors. *J. Virol.* **81,** 6548–62 (2007).

119. Li, Y. *et al.* Broad HIV-1 neutralization mediated by CD4-binding site antibodies. *Nat. Med.* **13,** 1032–4 (2007).

120. Blattner, C. *et al.* Structural delineation of a quaternary, cleavage-dependent epitope at the gp41-gp120 interface on intact HIV-1 Env trimers. *Immunity* **40,** 669–80 (2014).

121. Scharf, L. *et al.* Antibody 8ANC195 reveals a site of broad vulnerability on the HIV-1 envelope spike. *Cell Rep.* **7,** 785–95 (2014).

122. Piantadosi, A. *et al.* Breadth of neutralizing antibody response to human immunodeficiency virus type 1 is affected by factors early in infection but does not influence disease progression. *J. Virol.* **83,** 10269–10274 (2009).

123. Barouch, D. H. *et al.* Therapeutic efficacy of potent neutralizing HIV-1-specific monoclonal antibodies in SHIV-infected rhesus monkeys. *Nature* (2013). doi:10.1038/nature12744

124. Klein, F. *et al.* HIV therapy by a combination of broadly neutralizing antibodies in humanized mice. *Nature* **492,** 118–122 (2012).

125. Shingai, M. *et al.* Antibody-mediated immunotherapy of macaques chronically infected with SHIV suppresses viraemia. *Nature* **503,** 277–80 (2013).

126. Moldt, B. *et al.* Highly potent HIV-specific antibody neutralization in vitro translates into effective protection against mucosal SHIV challenge in vivo. *Proc. Natl. Acad. Sci.* **109,** 18921–18925 (2012).

127. Caskey, M. *et al.* Viraemia suppressed in HIV-1-infected humans by broadly neutralizing antibody 3BNC117. *Nature* (2015). doi:10.1038/nature14411

128. Scheid, J. F. *et al.* Sequence and structural convergence of broad and potent HIV antibodies that mimic CD4 binding. *Science* **333,** 1633–7 (2011).

129. Wu, X. *et al.* Focused evolution of HIV-1 neutralizing antibodies revealed by structures and deep sequencing. *Science* **333,** 1593–602 (2011).

130. Zhou, T. *et al.* Structural basis for broad and potent neutralization of HIV-1 by antibody VRC01. *Science* **329,** 811–7 (2010).

131. Zhou, T. *et al.* Multidonor analysis reveals structural elements, genetic determinants, and maturation pathway for HIV-1 neutralization by VRC01-class antibodies. *Immunity* **39,** 245–58 (2013).

132. Julien, J.-P. *et al.* Broadly neutralizing antibody PGT121 allosterically modulates CD4 binding via recognition of the HIV-1 gp120 V3 base and multiple surrounding glycans. *PLoS Pathog.* **9,** e1003342 (2013).

133. Liao, H.-X. *et al.* Co-evolution of a broadly neutralizing HIV-1 antibody and founder virus. *Nature* **496,** 469–76 (2013).

134. Doria-Rose, N. a *et al.* Developmental pathway for potent V1V2-directed HIV-neutralizing antibodies. *Nature* **509,** 55–62 (2014).

135. Moore, P. L. *et al.* Multiple pathways of escape from HIV broadly cross-neutralizing V2-dependent antibodies. *J. Virol.* **87,** 4882–94 (2013).

136. Kwong, P. D., Mascola, J. R. & Nabel, G. J. Broadly neutralizing antibodies and the search for an HIV-1 vaccine: the end of the beginning. *Nat. Rev. Immunol.* **13,** 693–701 (2013).

137. Haynes, B. F. *et al.* Progress in HIV-1 vaccine development. *J. Allergy Clin. Immunol.* **134,** 3–10 (2014).

138. Gao, F. *et al.* Cooperation of B Cell Lineages in Induction of HIV-1-Broadly Neutralizing Antibodies. *Cell* **158,** 481–491 (2014).

139. Garrett, N. J. *et al.* 004 Tenofovir Gel Pre-exposure Prophylaxis Trial. *J. Acquir. Immune Defic. Syndr.* **68,** 55–61 (2015).

140. Shuldiner, A. R., Tanner, K., Scott, L. A., Moore, C. A. & Roth, J. Ligase-free subcloning: a versatile method to subclone polymerase chain reaction (PCR) products in a single day. *Anal. Biochem.* **194,** 9–15 (1991).

141. Bryksin, A. & Matsumura, I. Overlap extension PCR cloning: a simple and reliable way to create recombinant plasmids. *Biotechniques* **48,** 463–465 (2011).

142. Gao, F. *et al.* Molecular cloning and analysis of functional envelope genes from human immunodeficiency virus type 1 sequence subtypes A through G. The WHO and NIAID Networks for HIV Isolation and Characterization. *J. Virol.* **70,** 1651–1667 (1996).

143. Hall, T. BioEdit: a user-friendly biological sequence alignment editor and analysis program for Windows 95/98/NT. *Nucleic Acids Symposium Series* **41,** 95–98 (1999).

144. Li, B. *et al.* Evidence for potent autologous neutralizing antibody titers and compact envelopes in early infection with subtype C human immunodeficiency virus type 1. *J. Virol.* **80,** 5211–5218 (2006).

145. Moore, P. L. *et al.* The c3-v4 region is a major target of autologous neutralizing antibodies in human immunodeficiency virus type 1 subtype C infection. *J. Virol.* **82,** 1860–9 (2008).

146. Gnanakaran, S. *et al.* Clade-specific differences between human immunodeficiency virus type 1 clades B and C: diversity and correlations in C3-V4 regions of gp120. *J. Virol.* **81,** 4886–91 (2007).

147. Pejchal, R. *et al.* A potent and broad neutralizing antibody recognized and penetrates the HIV glycan shield. *Science (80-.).* **1189,** 1097–1102 (2012).

148. Rong, R. *et al.* Escape from autologous neutralizing antibodies in acute/early subtype C HIV-1 infection requires multiple pathways. *PLoS Pathog.* **5,** e1000594 (2009).

149. Moore, P. L. *et al.* Limited neutralizing antibody specificities drive neutralization escape in early HIV-1 subtype C infection. *PLoS …* **5,** (2009).

150. Moore, P. L., Williamson, C. & Morris, L. Virological features associated with the development of broadly neutralizing antibodies to HIV-1. *Trends Microbiol.* **23,** 1–8 (2015).

151. Tomaras, G. D. *et al.* Polyclonal B Cell Responses to Conserved Neutralization Epitopes in a Subset of HIV-1-Infected Individuals. *J. Virol.* **85,** 11502–11519 (2011).

152. Wibmer, C. K. *et al.* Viral Escape from HIV-1 Neutralizing Antibodies Drives Increased Plasma Neutralization Breadth through Sequential Recognition of Multiple Epitopes and Immunotypes. *PLoS Pathog.* **9,** (2013).

153. Stamatatos, L., Morris, L., Burton, D. R. & Mascola, J. R. Neutralizing antibodies generated during natural HIV-1 infection: good news for an HIV-1 vaccine? *Nat. Med.* **15,** 866–870 (2009).

154. Derdeyn, C. a, Moore, P. L. & Morris, L. Development of broadly neutralizing antibodies from autologous neutralizing antibody responses in HIV infection. *Curr. Opin. HIV AIDS* **9,** 210–6 (2014).

155. Bhiman, J. N. *et al.* Viral variants that initiate and drive maturation of V1V2-directed HIV-1 broadly neutralizing antibodies. *Nat. Med.* **21,** 1–7 (2015).

156. Gray, E. S. *et al.* Neutralizing antibody responses in acute human immunodeficiency virus type 1 subtype C infection. *J. Virol.* **81,** 6187–96 (2007).

157. Lynch, R. M. *et al.* The B cell response is redundant and highly focused on V1V2 during early subtype C infection in a Zambian seroconverter. *J. Virol.* **85,** 905–915 (2011).

158. Georgiev, I. S. *et al.* Supplement: Delineating antibody recognition in polyclonal sera from patterns of HIV-1 isolate neutralization. *Science* **340,** 751–6 (2013).

159. Chenine, A. L. *et al.* Impact of HIV-1 backbone on neutralization sensitivity: Neutralization profiles of heterologous envelope glycoproteins expressed in native subtype C and CRF01-AE backbone. *PLoS One* **8,** 1–12 (2013).

160. van Gils, M. J. *et al.* Longer V1V2 region with increased number of potential N-linked glycosylation sites in the HIV-1 envelope glycoprotein protects against HIV-specific neutralizing antibodies. *J. Virol.* **85,** 6986–95 (2011).

161. Ferrari, G. *et al.* An HIV-1 gp120 envelope human monoclonal antibody that recognizes a C1 conformational epitope mediates potent antibody-dependent cellular cytotoxicity (ADCC) activity and defines a common ADCC epitope in human HIV-1 serum. *J. Virol.* **85,** 7029–7036 (2011).

162. Pincus, S. H. *et al.* Differences in the antibody response to human immunodeficiency virus-1 envelope glycoprotein (gp160) in infected laboratory workers and vaccinees. *J. Clin. Invest.* **91,** 1987–1996 (1993).

163. Buratti, E. *et al.* The neutralizing antibody response against a conserved region of human immunodeficiency virus type 1 gp41 (amino acid residues 731-752) is uniquely directed against a conformational epitope. *J. Gen. Virol.* **79 (Pt 11,** 2709–2716 (1998).

164. McLellan, J. S. *et al.* Structure of HIV-1 gp120 V1/V2 domain with broadly neutralizing antibody PG9. *Nature* **480,** 336–343 (2011).

165. Pancera, M. *et al.* Structural basis for diverse N-glycan recognition by HIV-1-neutralizing V1-V2-directed antibody PG16. *Nat. Struct. Mol. Biol.* **20,** 804–13 (2013).

166. Nelson, J. D. *et al.* An affinity-enhanced neutralizing antibody against the membrane-proximal external region of human immunodeficiency virus type 1 gp41 recognizes an epitope between those of 2F5 and 4E10. *J. Virol.* **81,** 4033–4043 (2007).

167. Julien, J.-P. *et al.* Crystal structure of a soluble cleaved HIV-1 envelope trimer. *Science* **342,** 1477–83 (2013).